SIMULATED LM STATIC REFLECTIVITY

DATA FOR SITE P-II-6*

By

H. S. Hayre, A. Tong and R. A. Meador

TR-67-21

Wave Propagation Laboratory
Department of Electrical Engineering

UNIVERSITY OF HOUSTON

Cullen College of Engineering
Cullen Boulevard
Houston, Texas 77004

November, 1967

*This work is sponsored by NASA - Manned Spacecraft Center, Houston, Texas, under Contract NAS-9-6760.

NASA CR 92483

SIMULATED LM STATIC REFLECTIVITY

DATE FOR SITE P-II-6

By

H. S. Hayre, A. Tong and R. A. Meador

ABSTRACT

A brief discussion of the LM acoustic simulation system and procedures used in taking static reflectivity data is given. A total of thirty points along the landing trajectory were selected for this data. The reflected field was plotted in dbs versus incident angles for quick reference.

THE SURFACE MODEL

The landing track with a length of 177 K feet is modeled on 36 feet long, 4 feet wide aluminum-base model composed of six sections 4' x 6' in size, as shown in Fig. 1 and Fig. 2. The scaling, design and construction have been reported in detail in a previous report (Hayre, Boyd and Tong, TR-67-6, 1967).

THE SELECTION OF POINTS

A total of 30 points were selected for the static data with appropriate consideration for low altitude effects. The distribution of the points along the landing trajectory is listed in Table 1 and shown in Fig. 3. Only a few data points were chosen at higher altitudes, whereas the point distribution along the trajectory becomes denser near the landing zone. The points were so chosen as to allow sufficient surface overlapping from one point to the next so that the whole track would be illuminated in subsequent look angles at various points. Furthermore, the reflectivity information is more critical at low altitude than it is at high altitude because of the smaller area illuminated at latter altitudes.

THE MODEL SURFACE MOUNTING

The model surface is attached to a fixed metal frame inside the water tank. The metal frame is mechanically isolated from other structures such that the experiment is noise free (vibration).

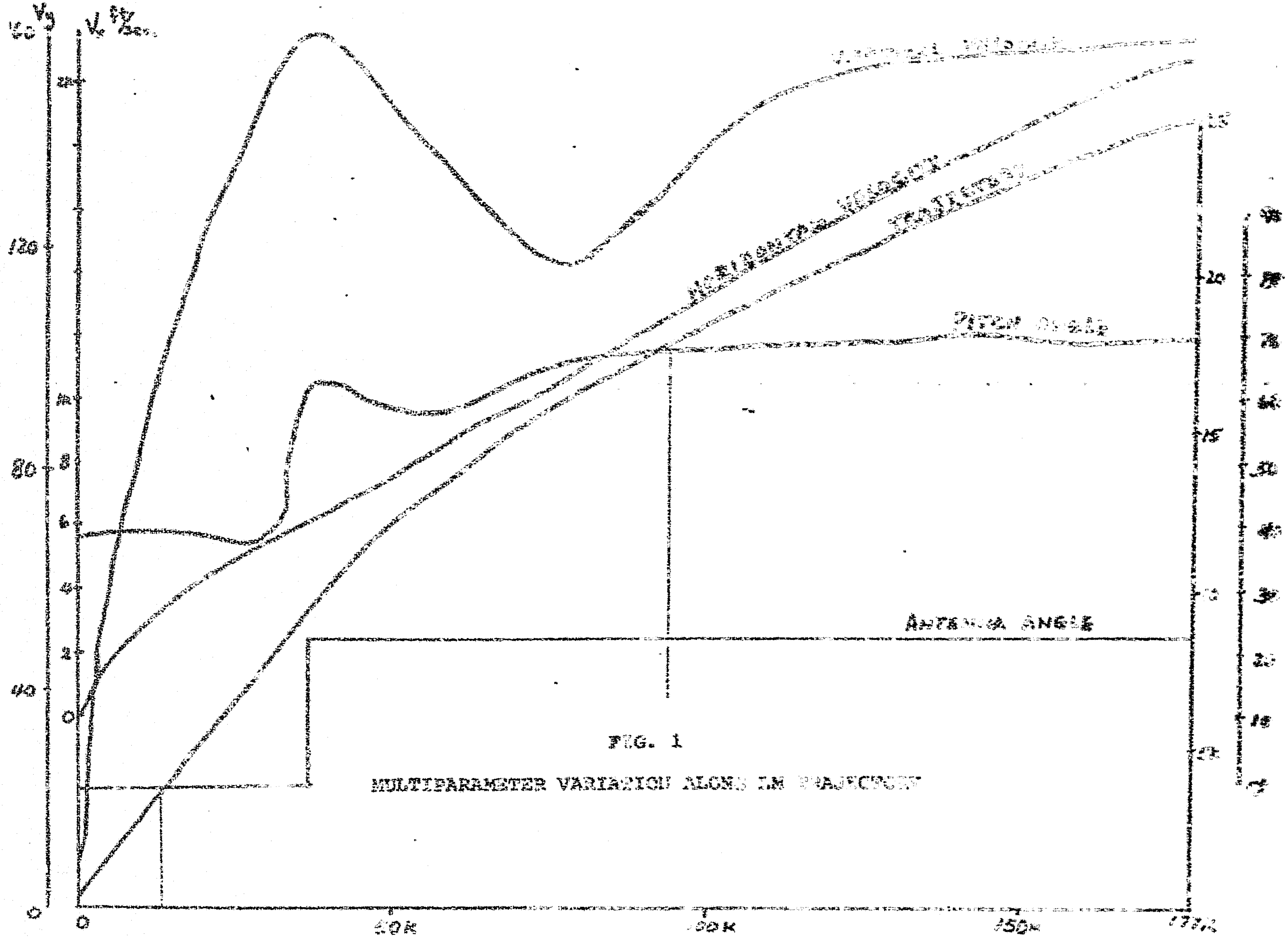

FIG. 1

MULTIPARAMETER VARIATION ALONG LM TRAJECTORY

DISTANCE (x',x) FROM CENTER OF LANDING ELLIPSE

	x ft.	x' in.	y ft.	y' in.
1	177 K	143.7372	25000	43.7956
2	150 K	95.3504	23000	40.2920
3	125 K	52.5547	20800	36.4380
4	107.5 K	21.8978	19200	33.6350
5	100 K	8.7591	18400	32.2336
6	95 K	0.0	17950	31.4453
7	95 K	143.7372	17950	31.4453
8	88.5 K	132.3504	17300	30.3066
9	78.3 K	113.9562	16200	28.3795
10	75 K	108.7007	15800	27.6788
11	53.9 K	71.9124	12800	22.4236
12	36.2 K	40.7299	9250	16.2046
13	34.9 K	38.4526	8938	15.6578
14	33.7 K	36.3504	8622	15.1042
15	32.[illegible] K	34.2482	8310	14.5577
16	27.9 K	26.1800	7150	12.5255
17	25 K	21.1095	6500	11.3869
18	22.8 K	17.3888	5870	10.2832
19	18.3 K	9.3723	4800	8.4008
20	14.4 K	2.5401	3800	6.6569
21	12.95K	0.0	3400	5.9562
22	12950	143.8896	3400	37.7778
23	11000	122.2222	3000	33.3333
24	8100	90.0000	2300	25.5556
25	5740	63.7778	1760	19.5556
26	3870	43.0000	1290	14.3333
27	2430	27.0000	900	10.0000
28	1720	19.0000	700	7.7778
29	1380	15.3333	600	6.6667
30	740	8.2222	400	4.4444
31	670	7.4444	373	4.1444
32	246	2.7333	220	2.4444
33	195	2.1667	200	2.2222

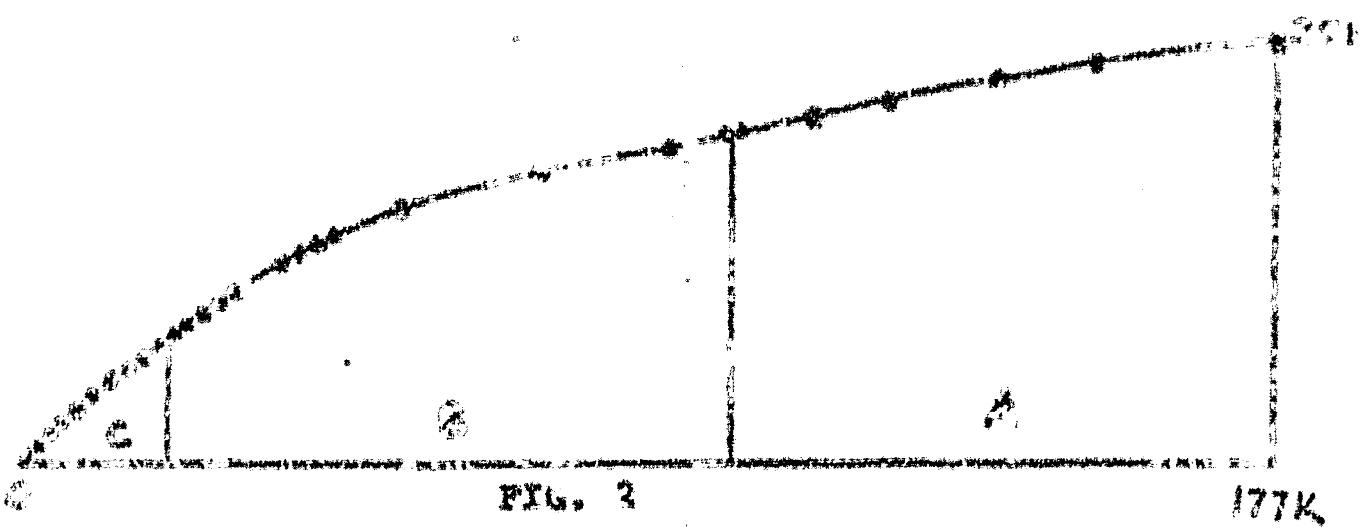

FIG. 2

TRAJECTORY AND LOCATION OF STATIC DATA ROOMS

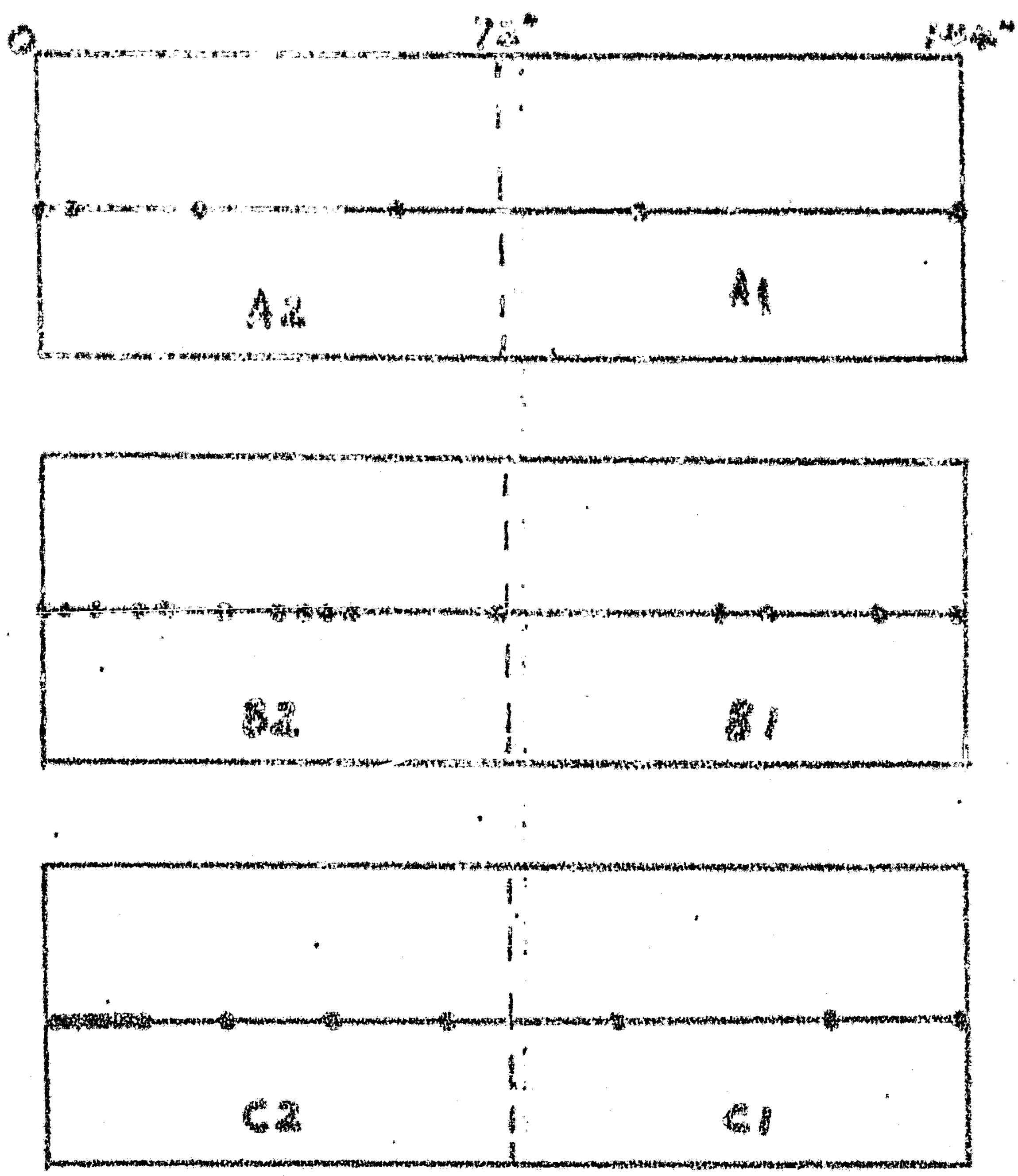

FIG. 3

DATA-POINTS ON THE TRAJECTORY

THE TRANSMITTER AND RECEIVER MOUNTING

The transmitter and receiver are mounted on a rigid arm attached to a motor carrier. The carrier and the surface frame have the same mechanical reference so that any vibration will be self-cancelled.

THE POSITIONING OF THE TRANSMITTER AND RECEIVER

The X (lateral distance measured from the center of the landing zone) and Y (altitude from the lunar surface) position of the carrier are controlled by DC motors which have built-in mechanical feedback. These position reading signals are fed into digital encoders with a readout accuracy up to a hundredth of an inch. The angular control of the transmitter and receiver is designed to change one degree per pulse input. The angular swing is from 0° to 70° toward the landing, as shown in Fig. 4. Figure 5 shows the overall electrical and mechanical layout of the entire system.

DATA

A sample of raw data is presented in Fig. 6 where the return signal envelope is plotted. The incident angle of the transmitter corresponds to the number of pulses and is also recorded in the same graphs. Fig. 7 through Fig. 36 are the return signal in dbs plotted versus the incident angle of the transmitter and has a resolution of 1 degree.

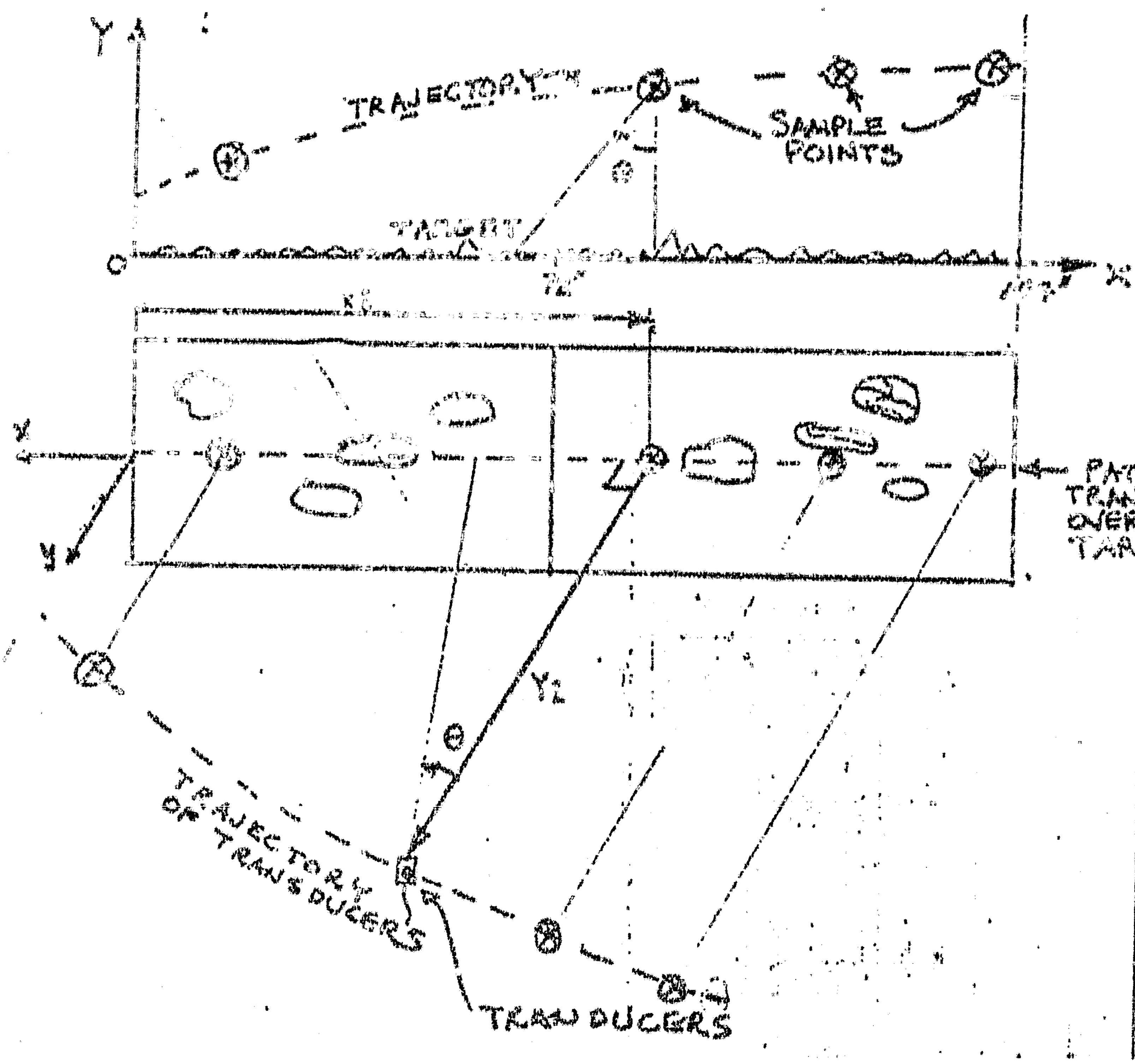

FIG. 6

OVER VIEW OF THE RELATIVE LOCATIONS OF LM SIMULATED RADAR PACKAGE AND TARGET SURFACE

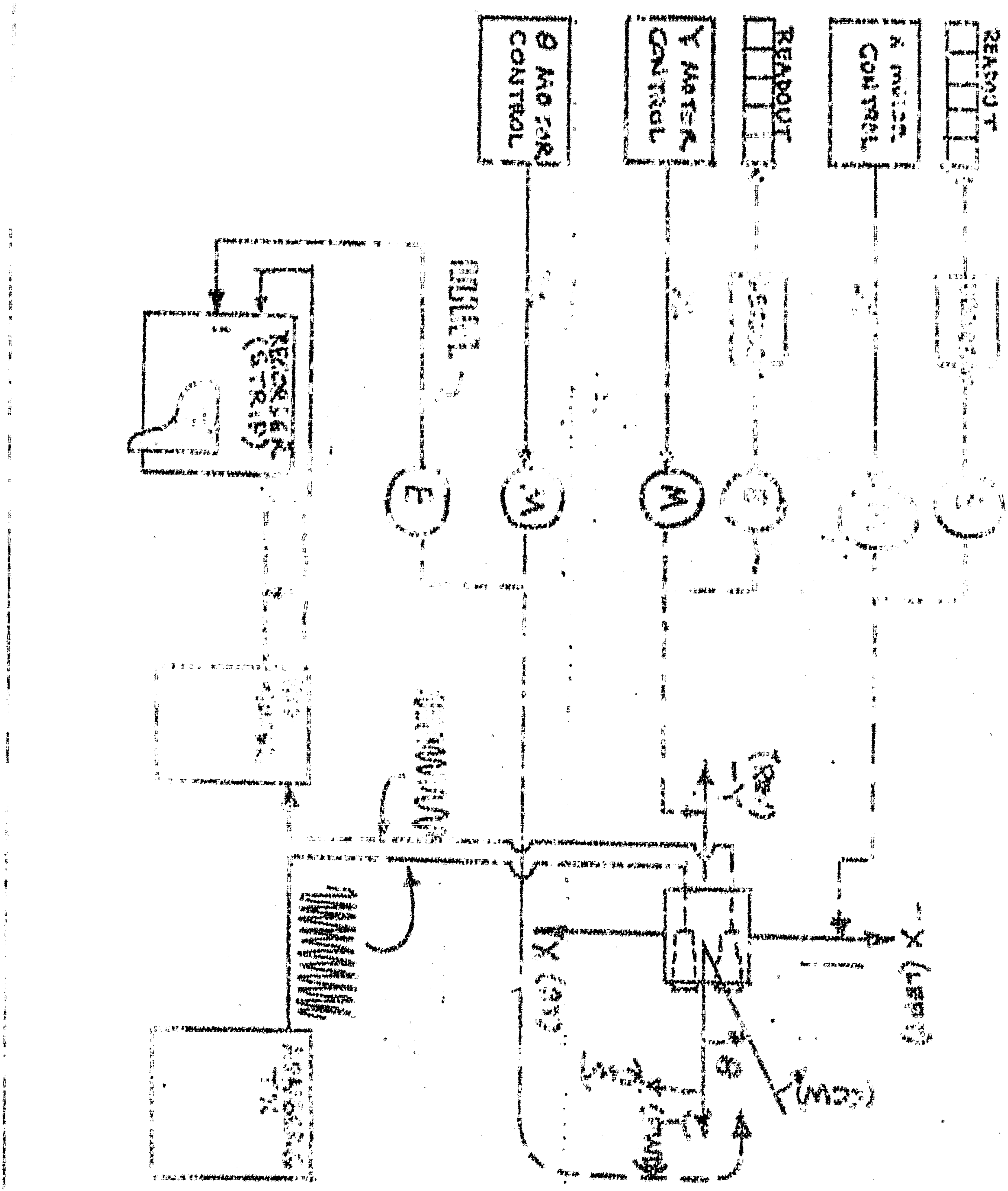

FIG. 5

BLOCK DIAGRAM OF INSTRUMENTATION FOR STATIC LM LANDING SIMULATION

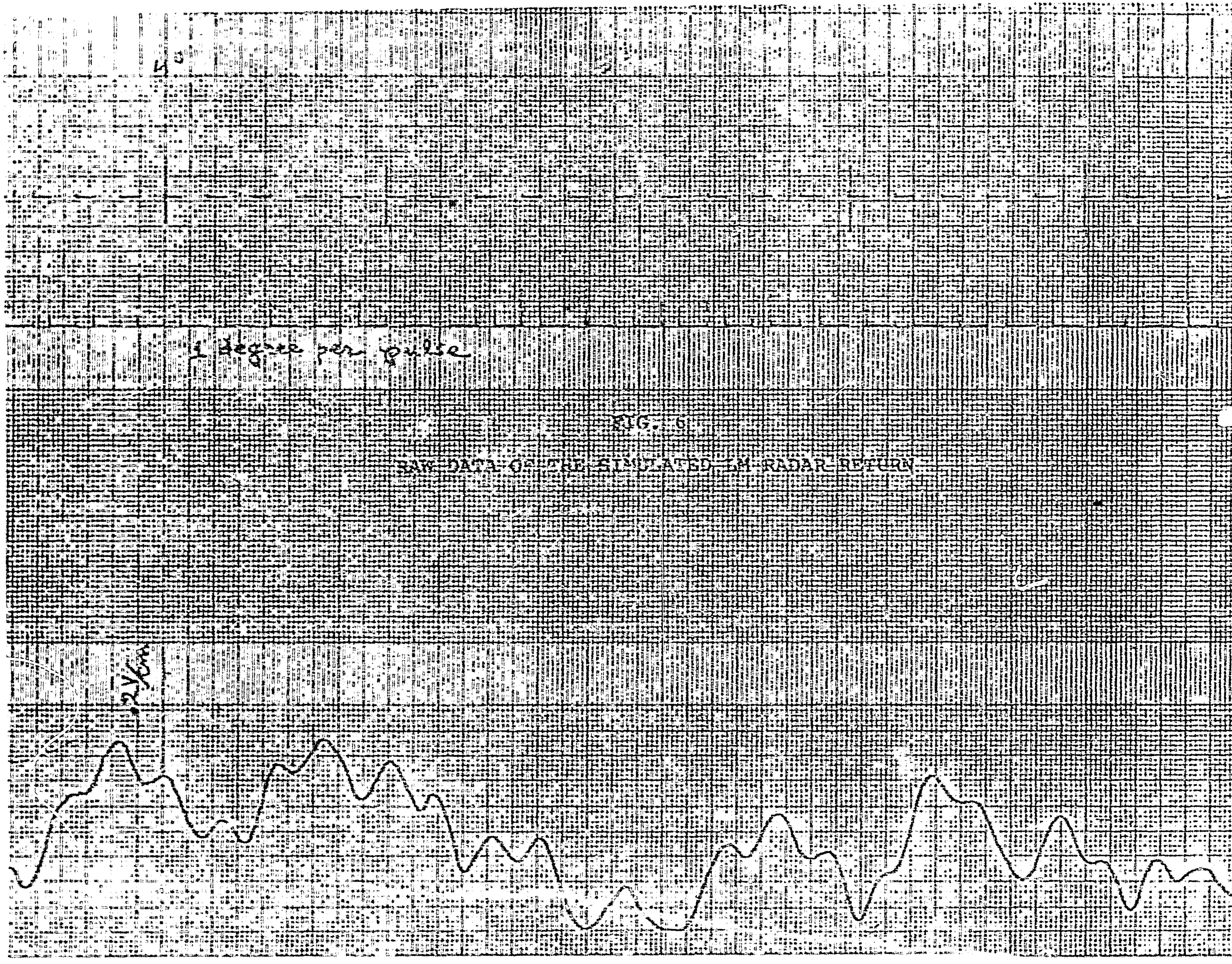

FIG. 6

RAW DATA OF THE SIMULATED LM RADAR RETURN

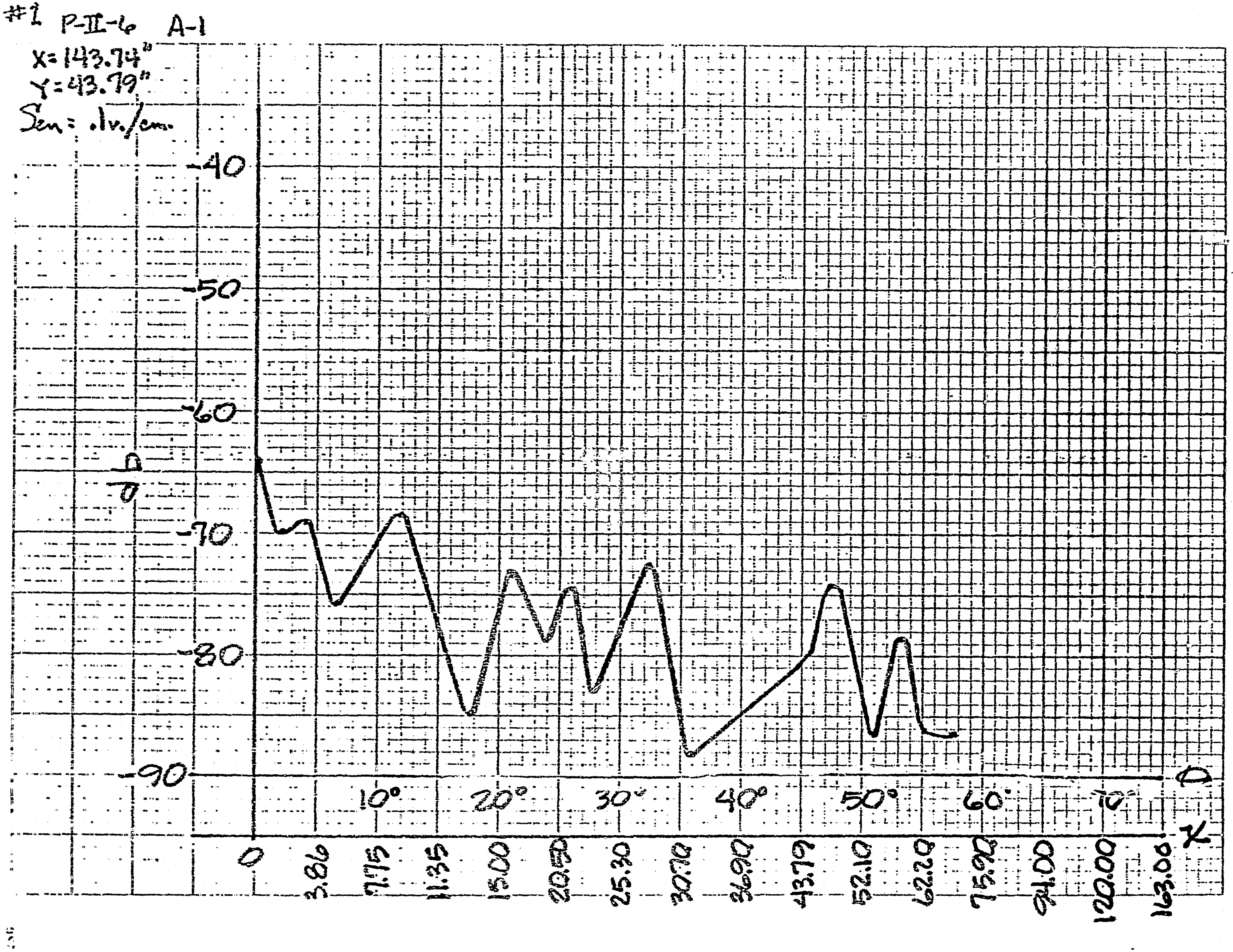
#1 P-II-6 A-1
X=143.74"
Y=43.79"
Sen = .1v./cm.
-40
-50
-60
-70
-80
-90
10°
20°
30°
40°
50°
60°
70°
0
3.86
7.75
11.35
15.00
20.50
25.30
30.70
36.90
43.79
52.10
62.20
75.90
94.00
120.00
163.00
K

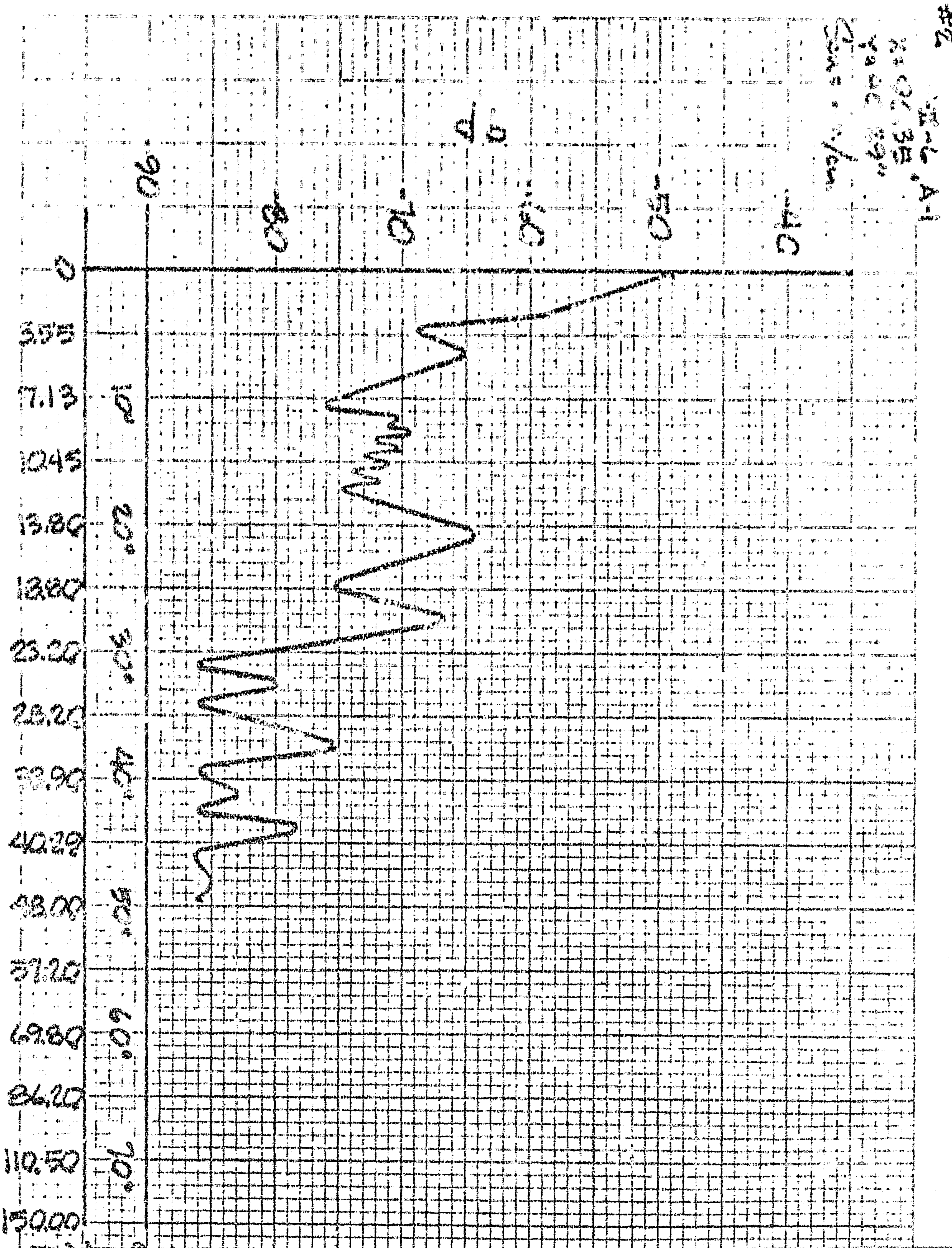

90
80
70
60
50
40
0
3.55
7.13
10.45
13.80
23.20
28.20
33.90
40.29
48.00
57.20
69.80
86.20
110.50
150.00
10°
20°
30°
40°
50°
60°
70°

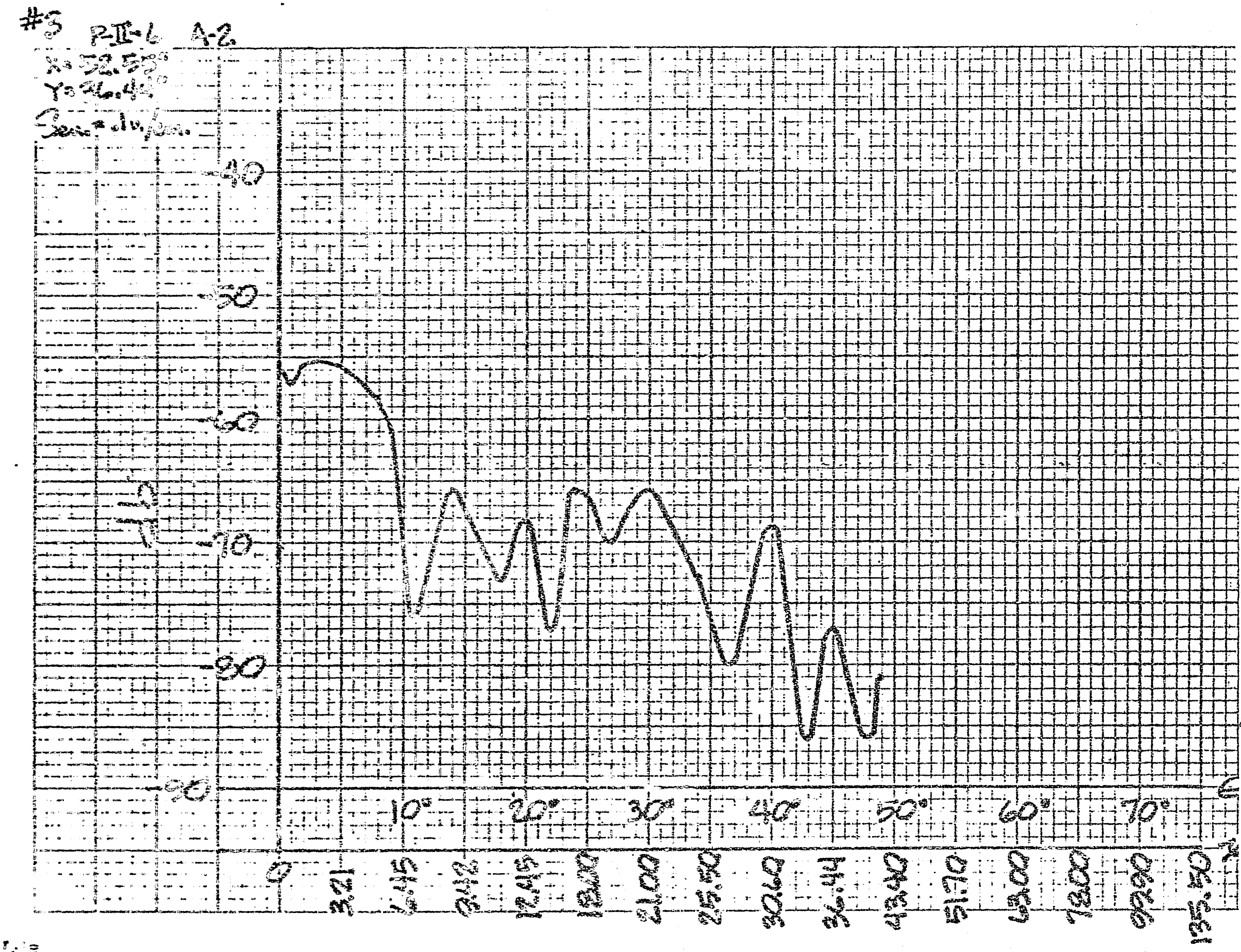

#5 P-II-6 A-2
X = 52.55°
Y = 76.42°
Sens = .1v/cm.
dB
-40
-50
-60
-70
-80
-90
0
10°
20°
30°
40°
50°
60°
70°
3.21
6.45
9.42
12.45
18.00
21.00
25.50
30.60
36.44
43.40
51.70
63.00
78.00
99.90
135.50

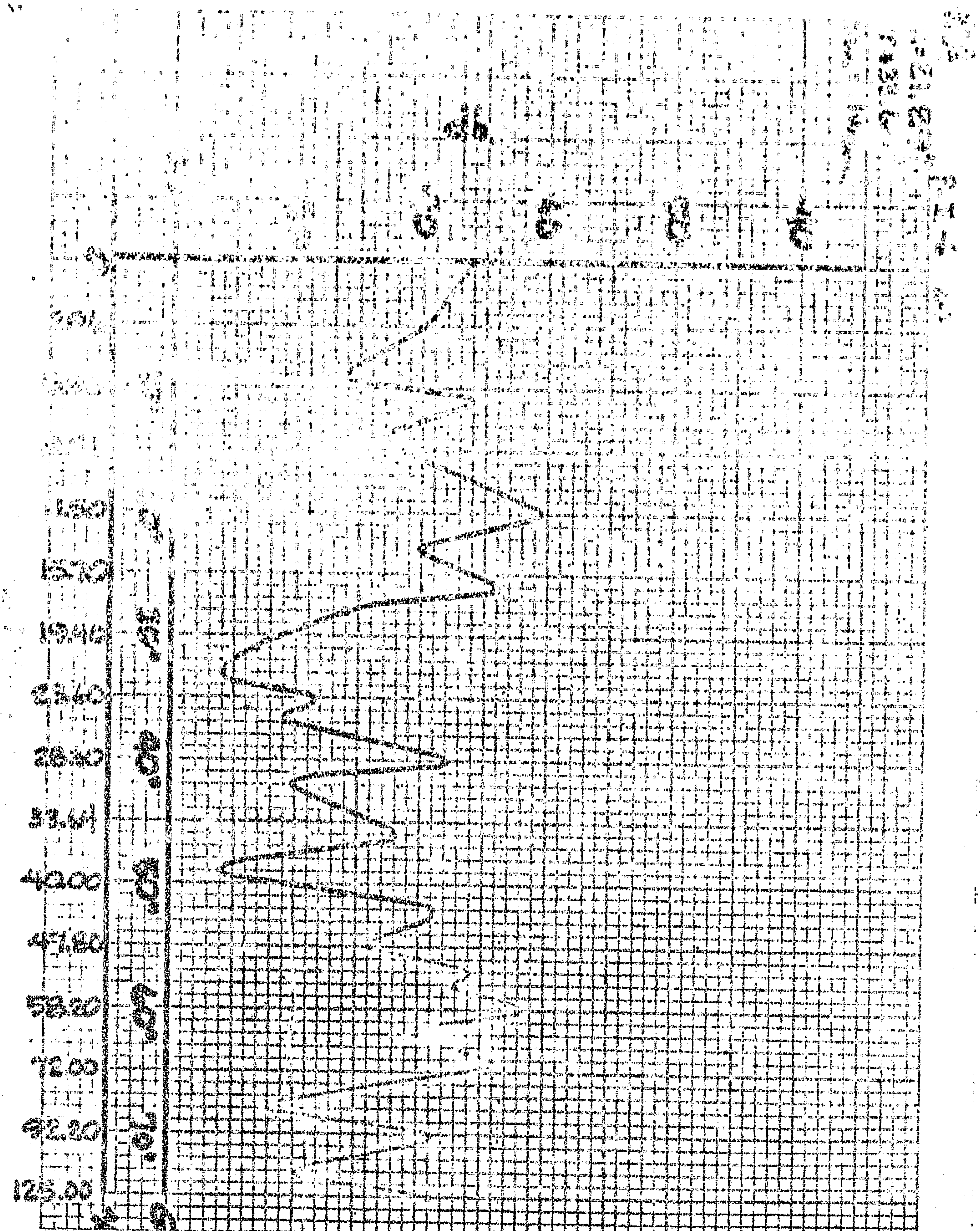
40.00
47.80
58.20
72.00
92.20
125.00

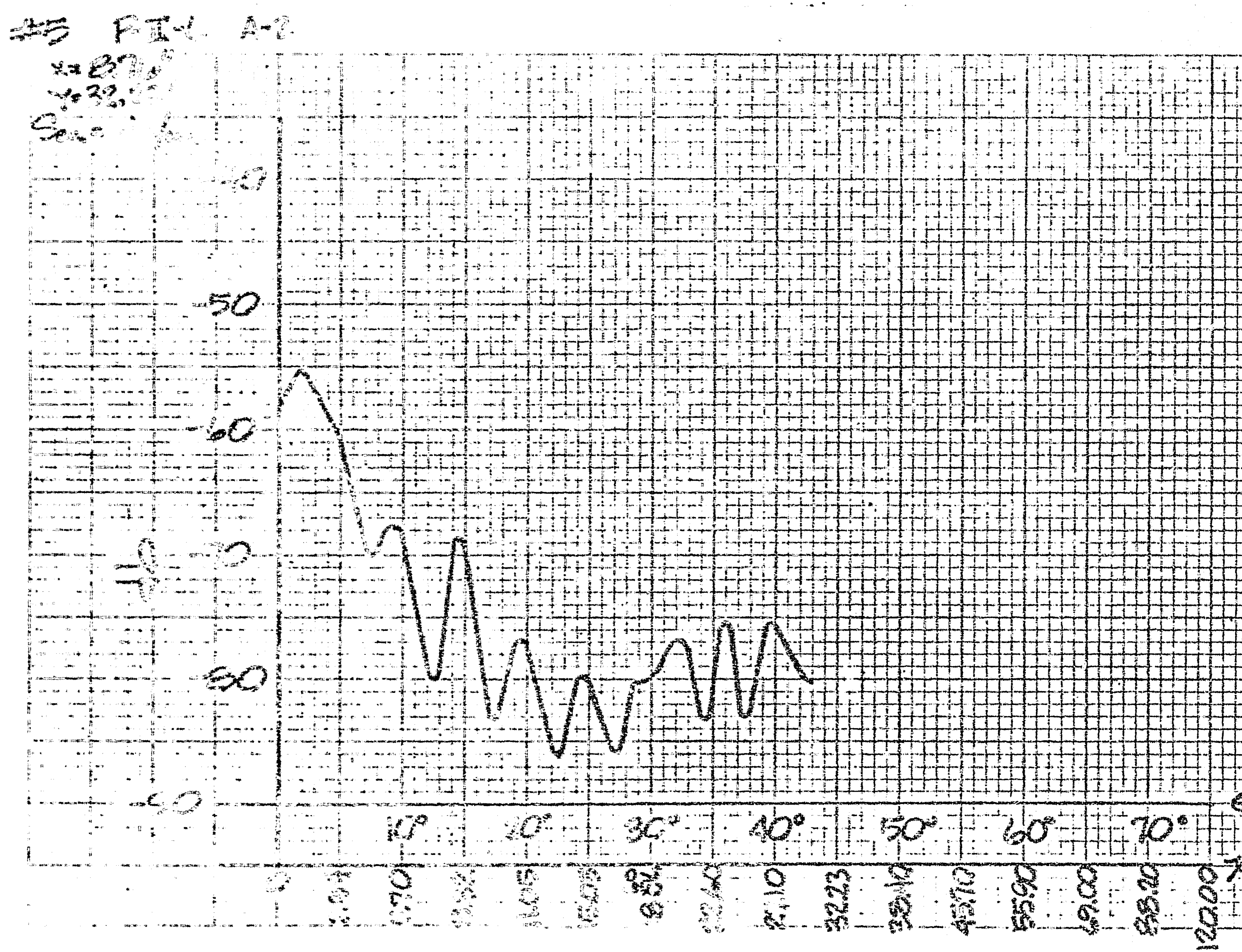
#5 PI-1 A-2
-50
-60
-80
10°
20°
30°
40°
50°
60°
70°
32.23
45.10
55.90
69.00
88.20
120.00

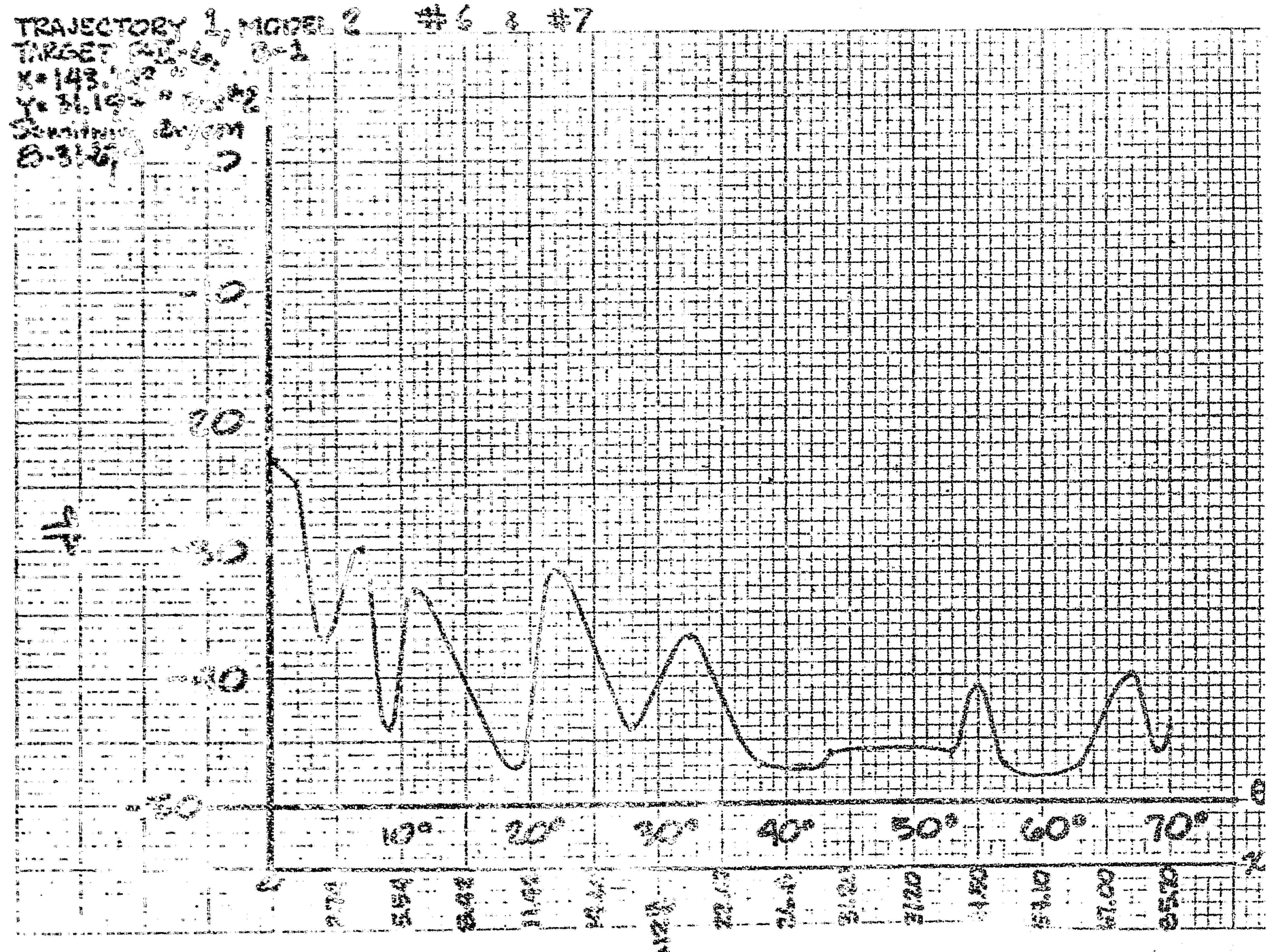

TRAJECTORY 1, MODEL 2 #6 & #7
0
10
20
30
40
50
60
70
10°
20°
30°
40°
50°
60°
70°

TRAJECTORY 1, MODEL 2 #8
TARGET R-II-6 B-1
X= 132.330"
Y= 30.038"
Sensitivity=.2v/cm
8-31-63

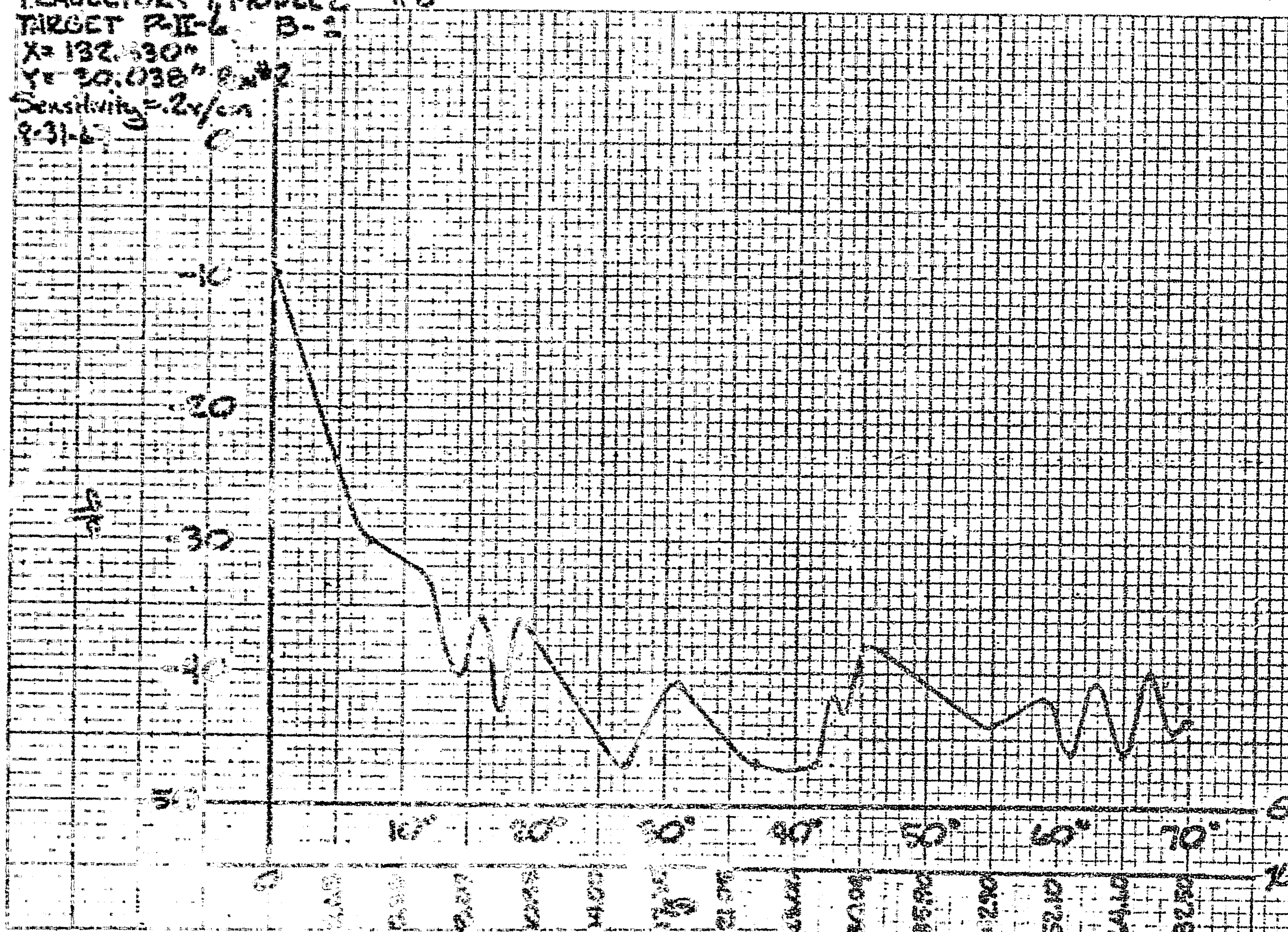

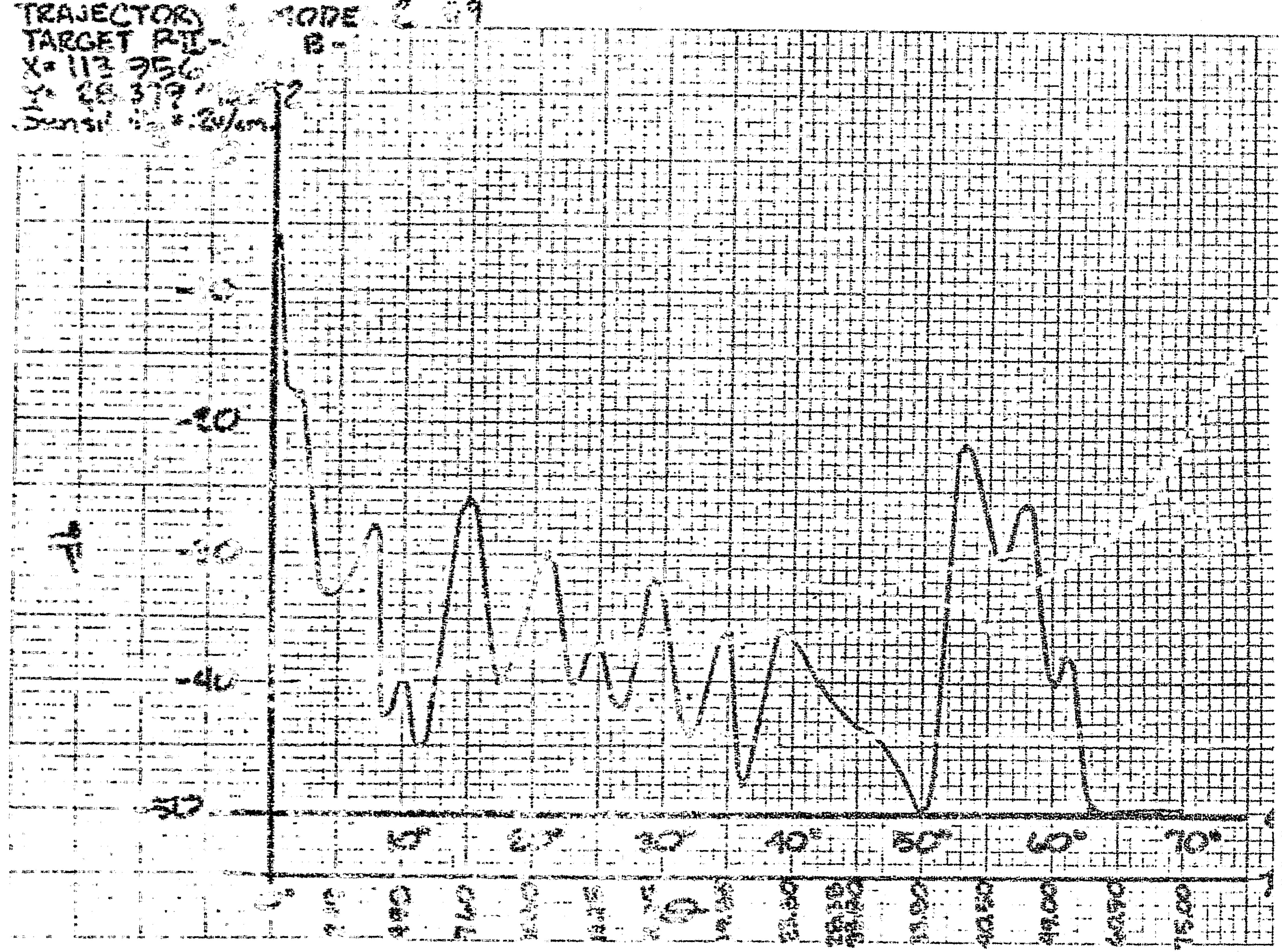
TRAJECTORY MODE
TARGET
-20
-30
-40
10°
20°
30°
40°
50°
60°
70°
40.50
75.00

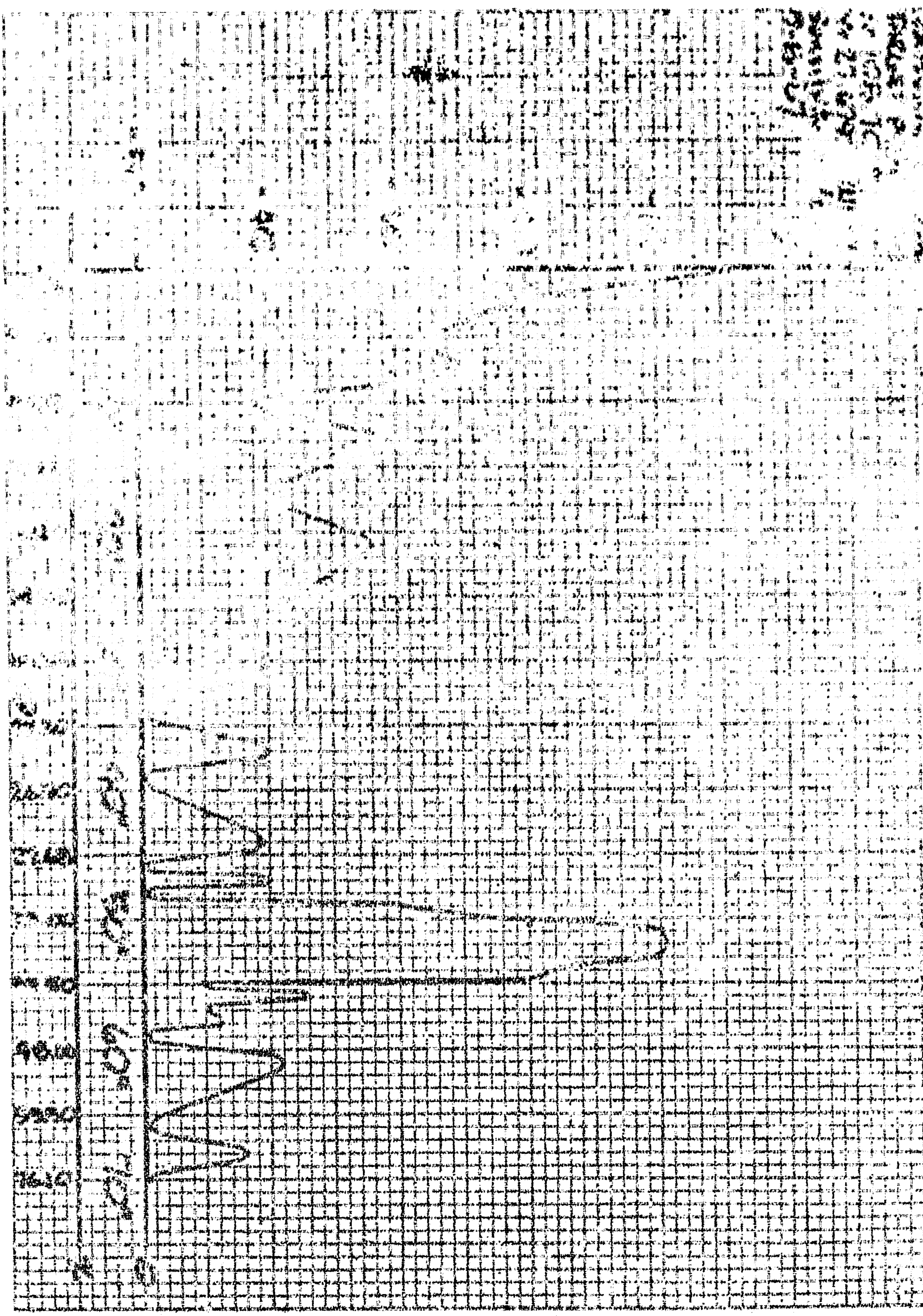

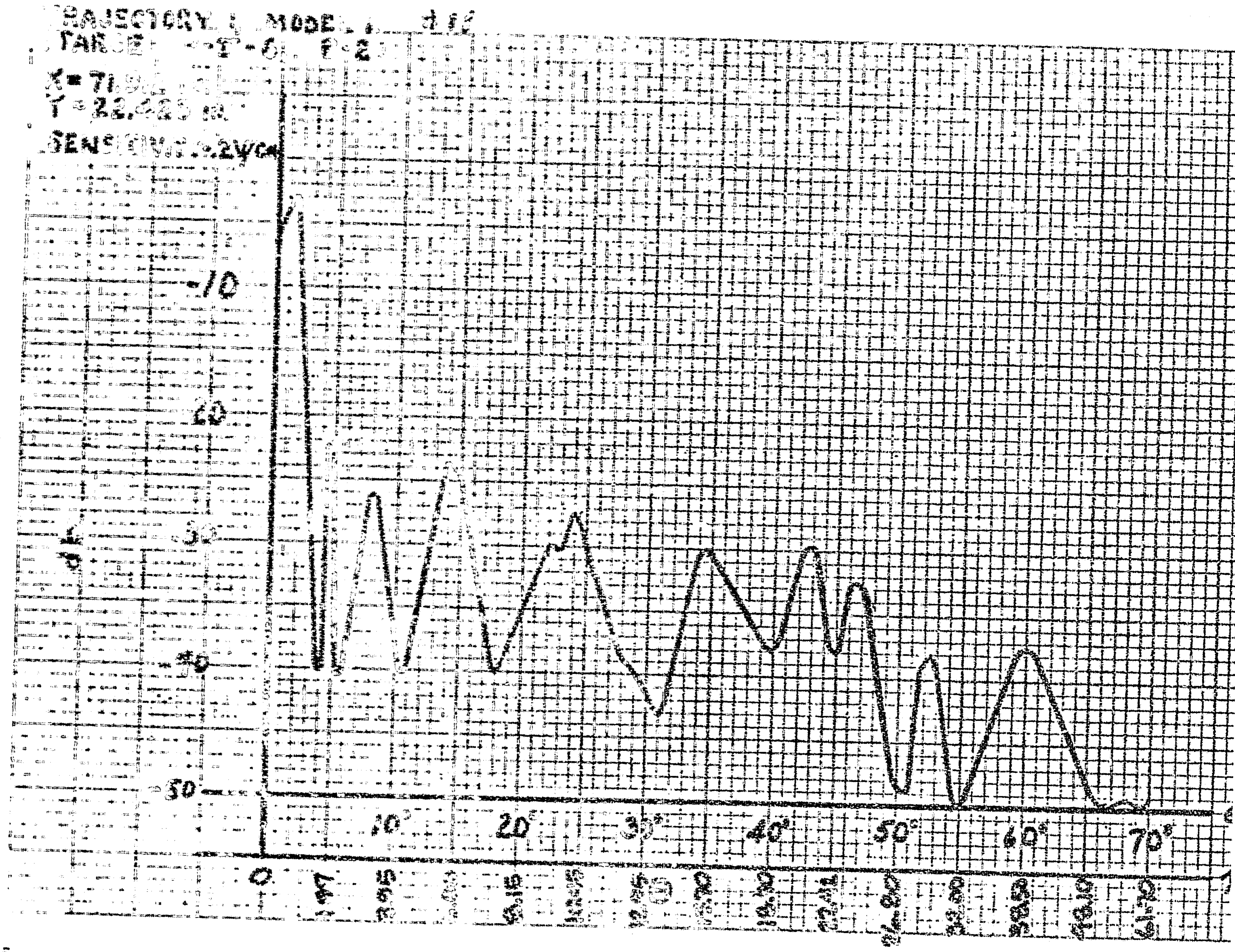
TRAJECTORY MODEL
TARGET T-6 P-2
SENSITIVITY 2V/CM
10
20
30
40
50
0
10°
20°
30°
40°
50°
60°
70°

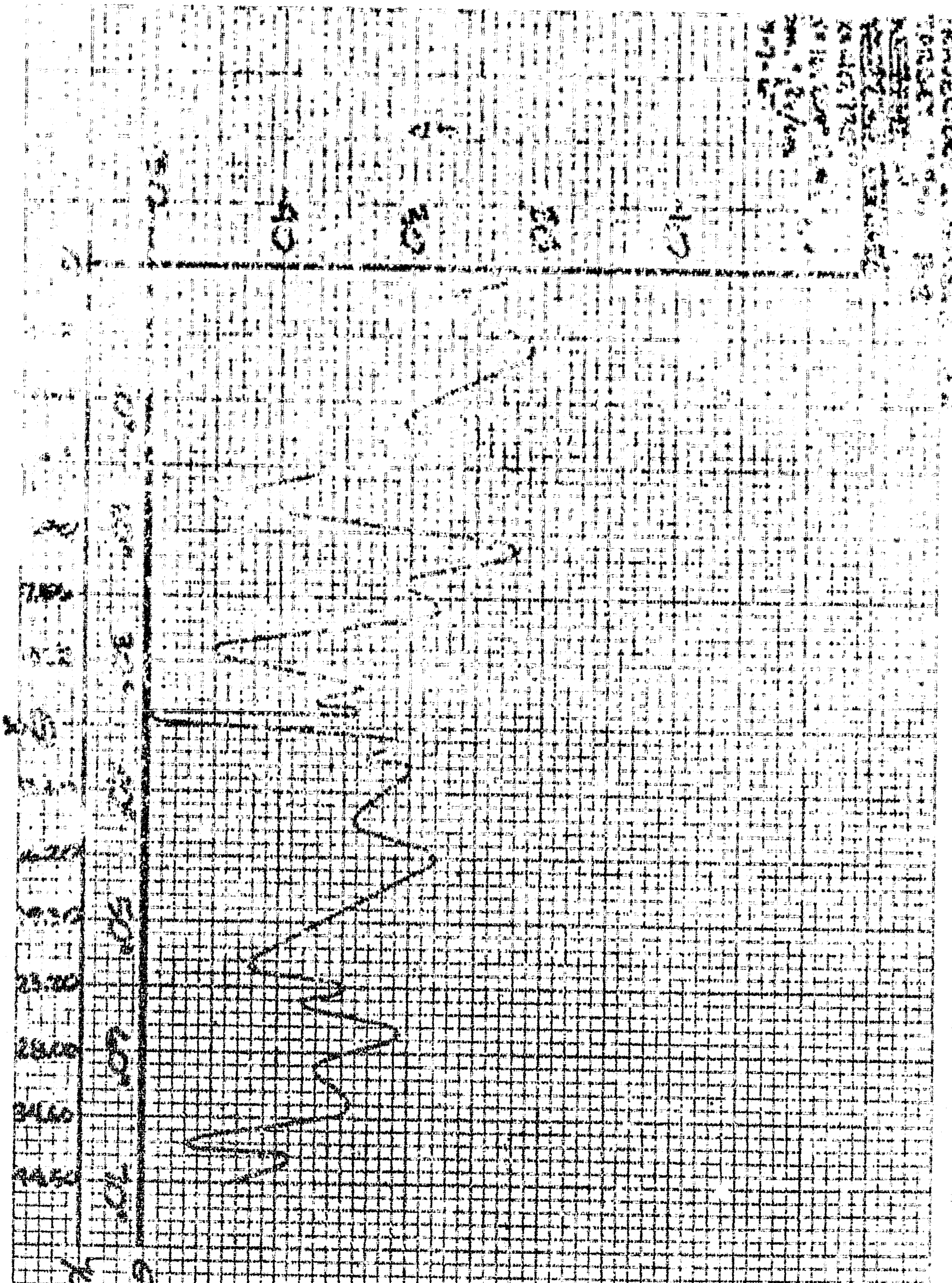

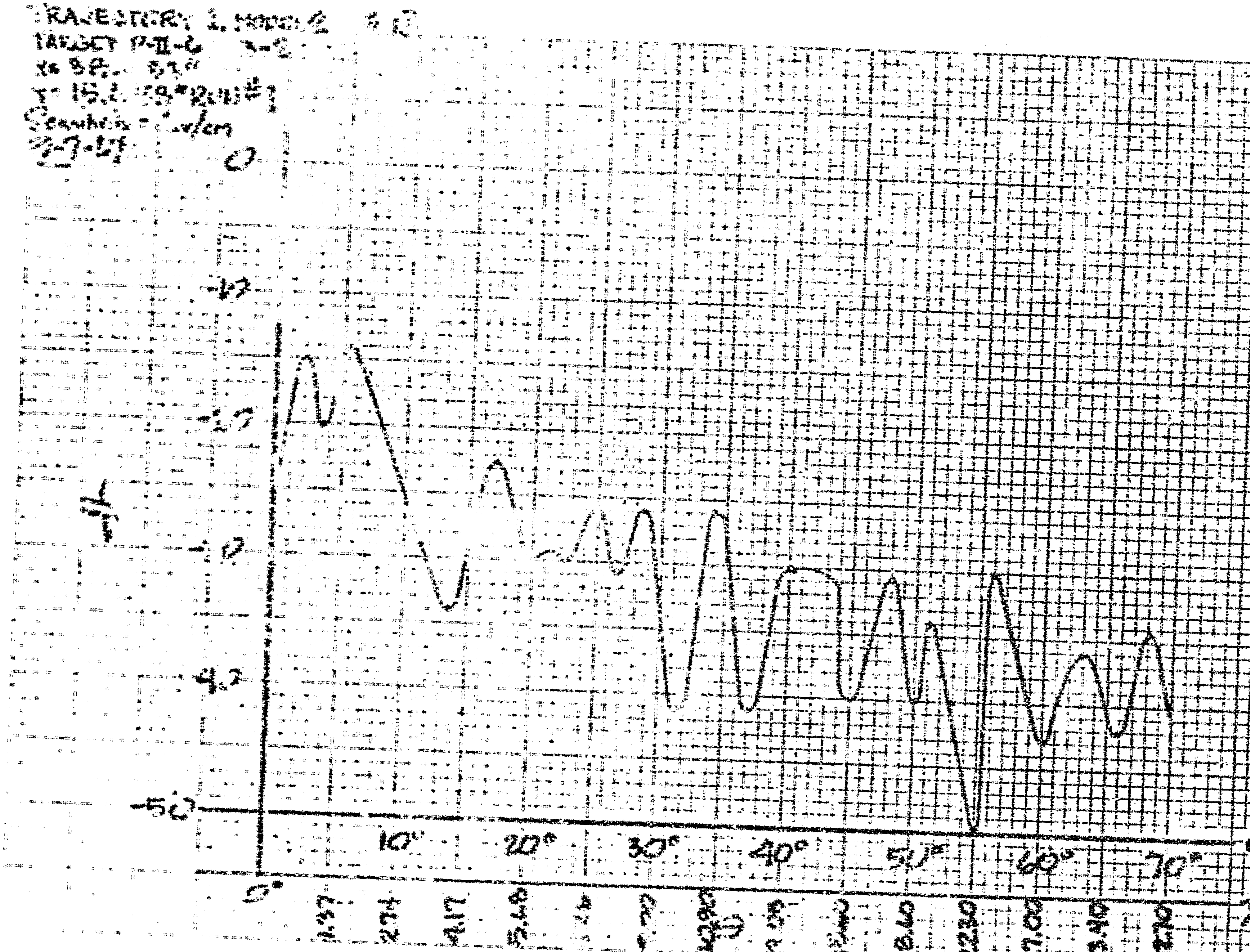
TRAJECTORY 1, MODE 2
TARGET P-II-6

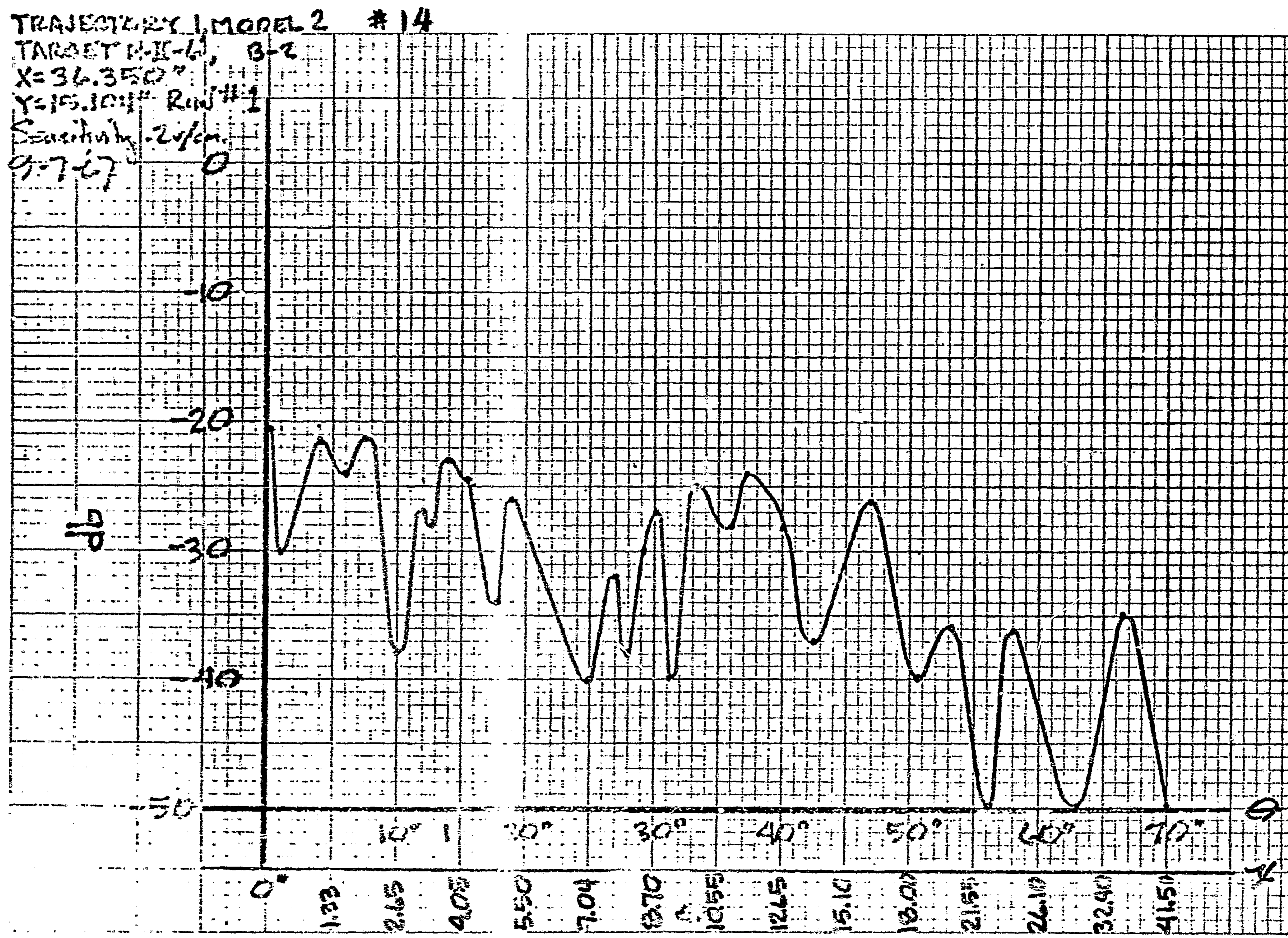

TRAJECTORY 1, MODEL 2 #14
TARGET N-II-6, B-2
X=36.350"
Y=15.104" Run #1
Sensitivity .2v/cm.
9-7-67
db
0
-10
-20
-30
-40
-50
θ
10°
20°
30°
40°
50°
60°
70°
0"
1.33
2.65
4.05
5.50
7.04
8.70
10.55
12.65
15.10
18.00
21.55
26.10
32.90
41.50

TRAJECTORY 1, MODEL 2 #15
TARGET P-II-6, B-2
X = 34.248"
Y = 14.553" mid #2
Sensitivity .2v/cm.

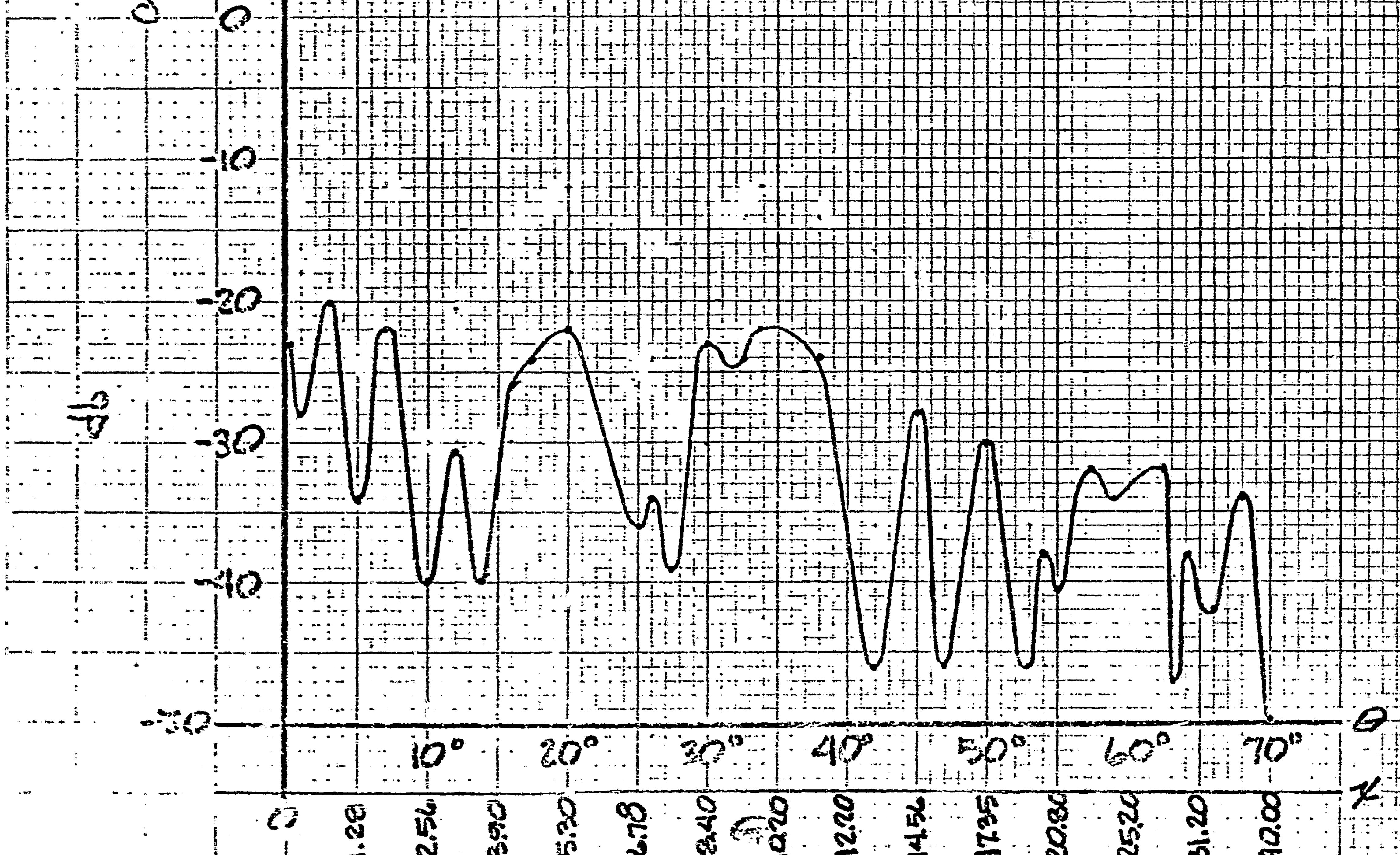

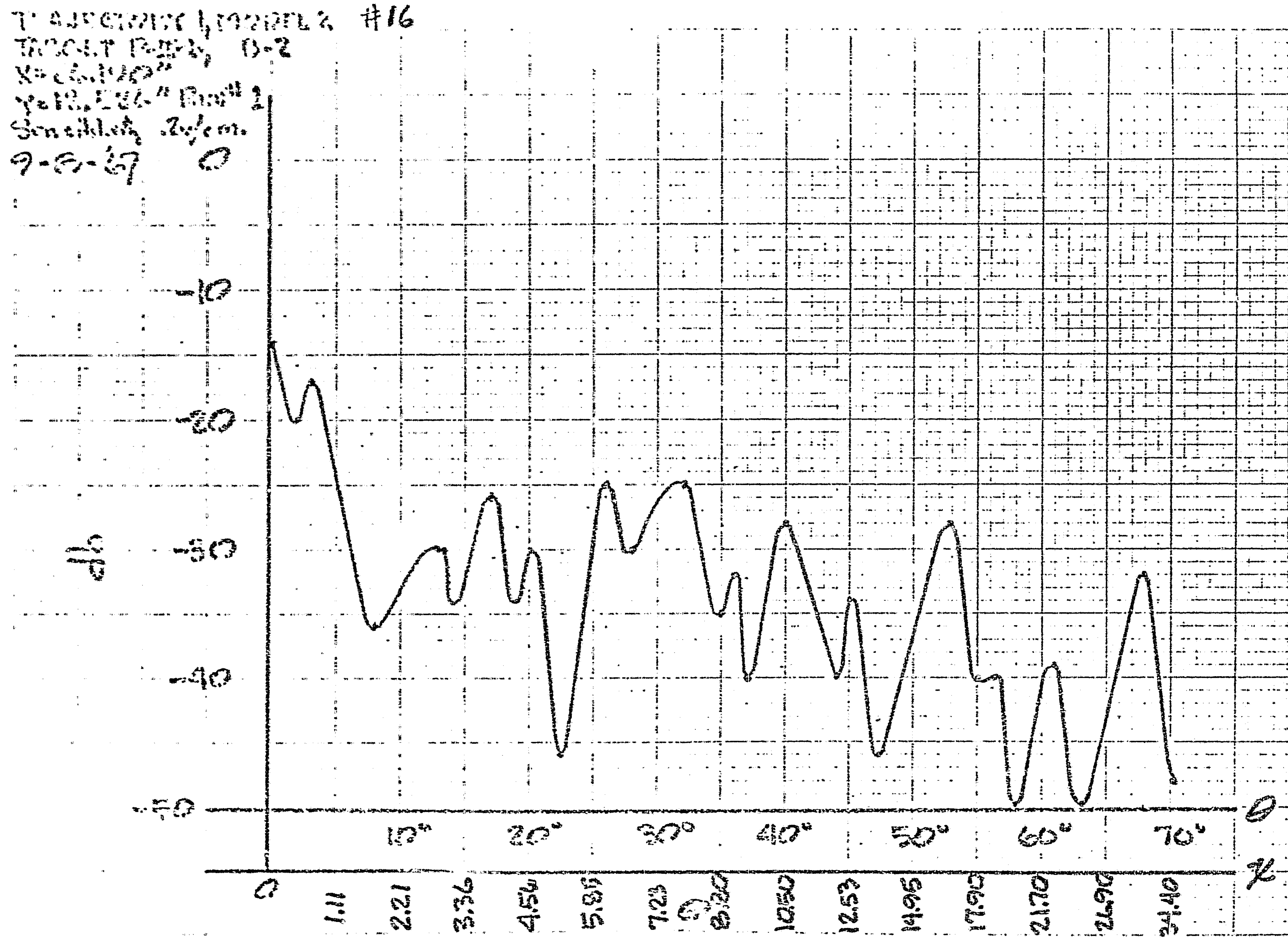
#16
D-2
9-6-67
db
0
-10
-20
-30
-40
-50
0
10°
20°
30°
40°
50°
60°
70°
0
1.11
2.21
3.36
4.56
5.85
7.23
8.20
10.50
12.53
14.95
17.90
21.70
26.90
34.40

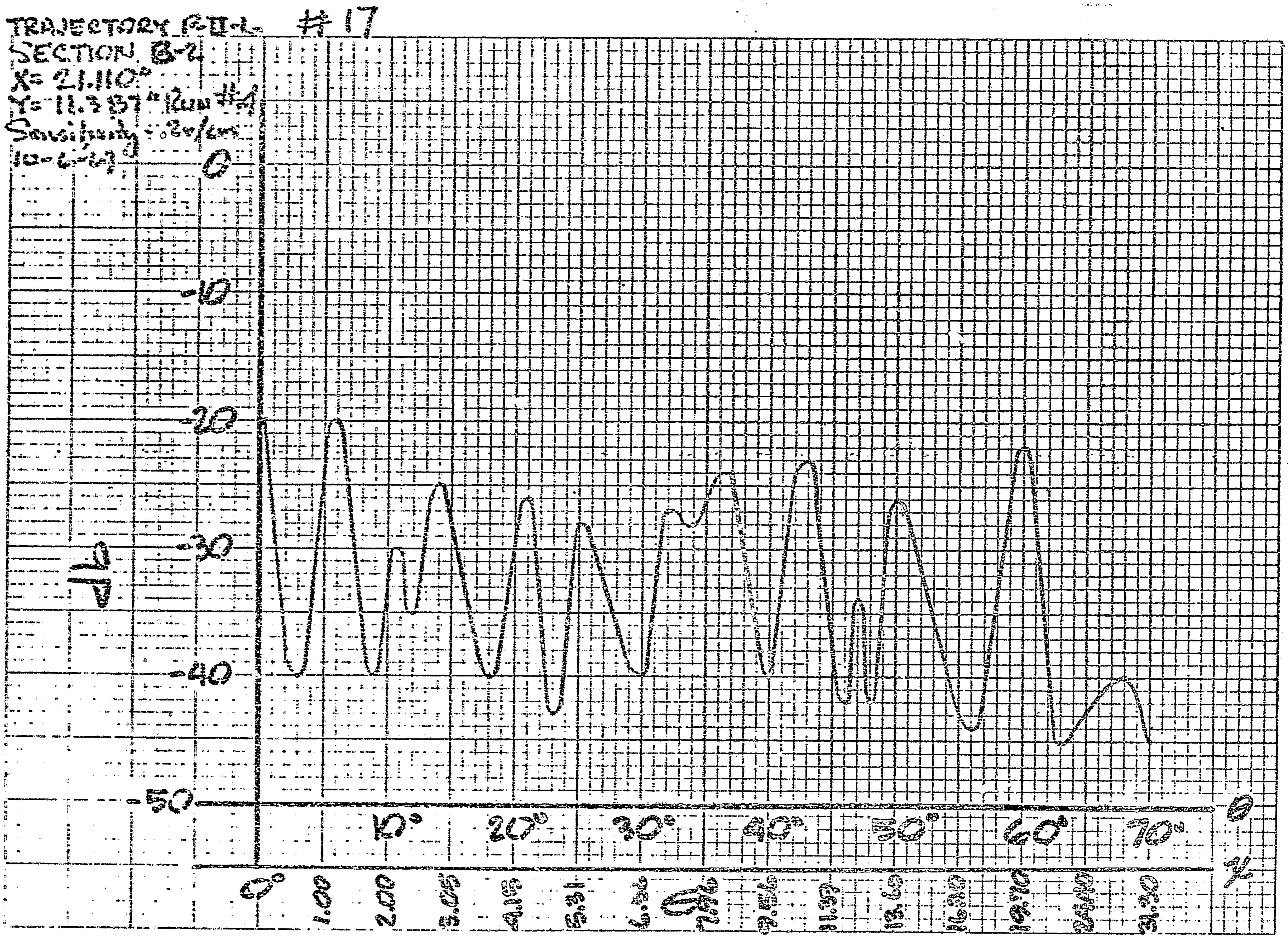
TRAJECTORY G-II-L #17
SECTION B-2
X= 21.110"
Y= 11.387" Run #4
Sensitivity: .2v/cm
10-6-67
dB
0
-10
-20
-30
-40
-50
10°
20°
30°
40°
50°
60°
70°
0
θ
0°
1.00
2.00
3.05
4.15
5.31
6.56
7.96
9.56
11.39
13.60
16.30
19.70
24.40
31.30
γ

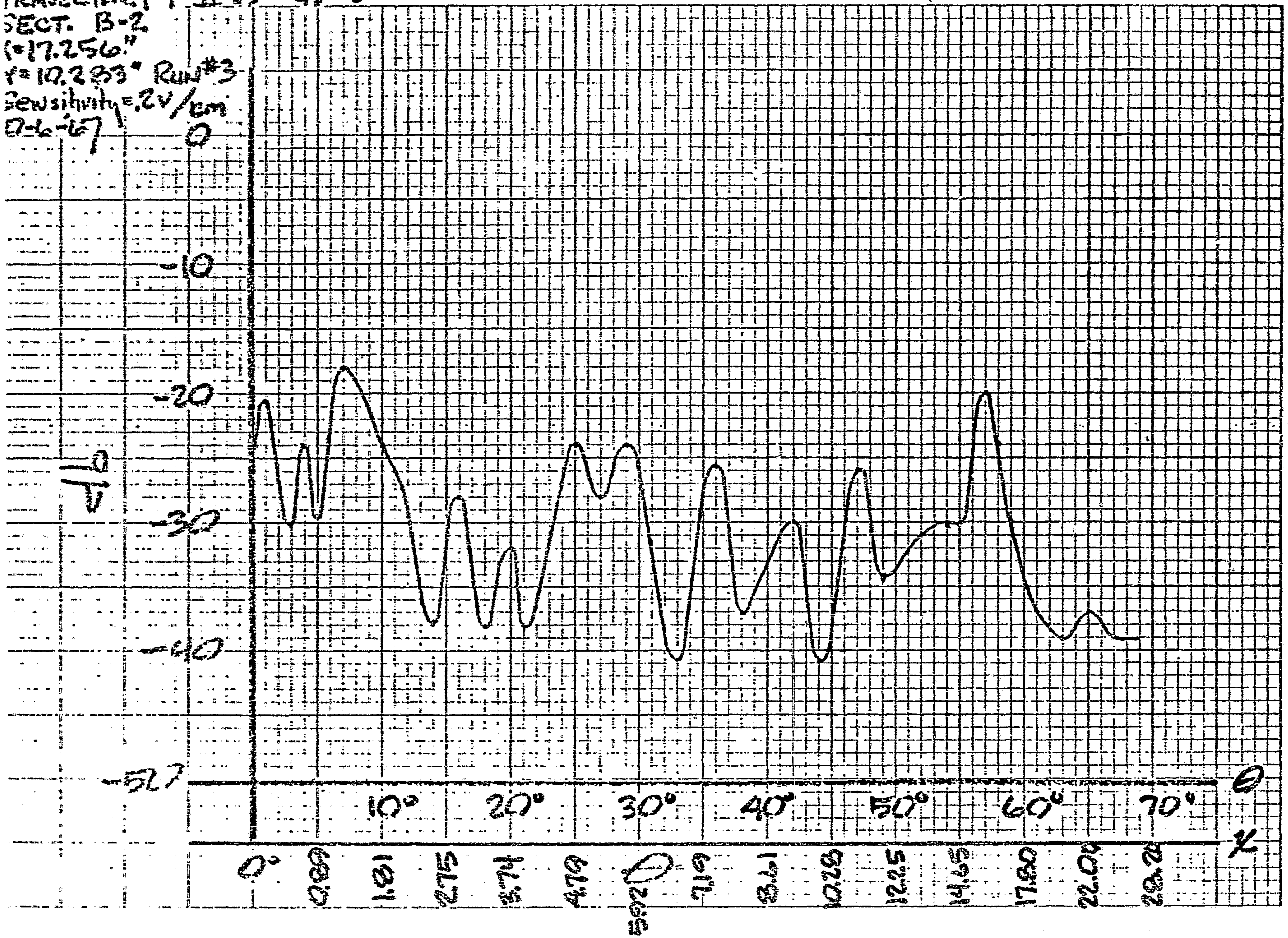
SECT. B-2
x=17.256"
y=10.283" Run #3
Sensitivity=.2V/cm
12-6-67
0
-10
-20
-30
-40
-52.7
10°
20°
30°
40°
50°
60°
70°
θ
x
0°
0.89
1.81
2.75
3.74
4.79
5.92
7.19
8.61
10.28
12.25
14.65
17.80
22.04
28.20

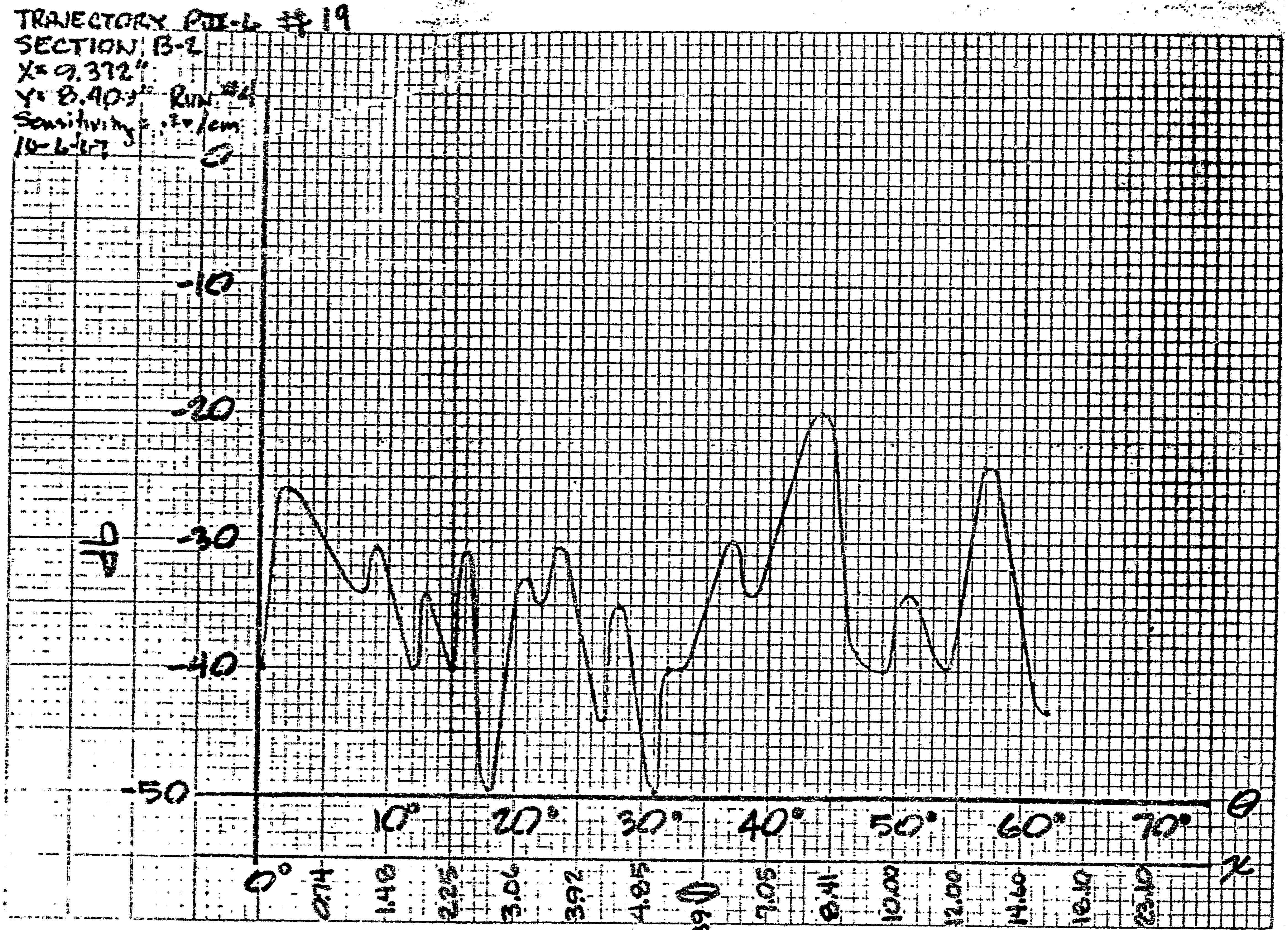
TRAJECTORY PIII-6 #19
SECTION B-2
X= 9.372"
Y= 8.403" RUN #4
Sensitivity .2v/cm
10-6-47
dB
-10
-20
-30
-40
-50
0
10°
20°
30°
40°
50°
60°
70°
θ
0°
0.74
1.48
2.25
3.06
3.92
4.85
5.89
7.05
8.41
10.00
12.00
14.60
16.10
23.10
x

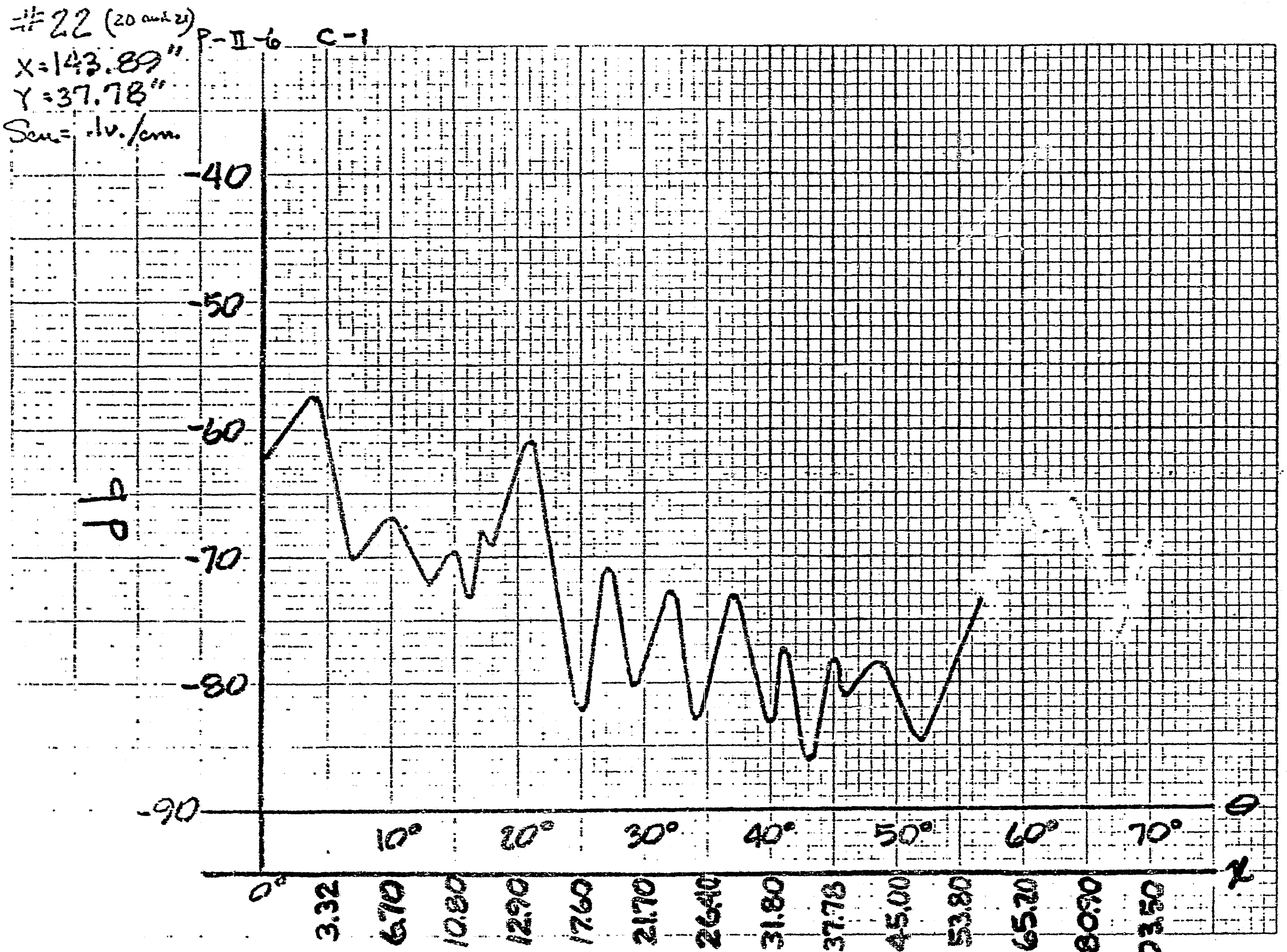

#22 (20 and 21) P-II-6 C-1
X=143.89"
Y=37.78"
Sen= .1v./cm.
db
-40
-50
-60
-70
-80
-90
0°
10°
20°
30°
40°
50°
60°
70°
θ
3.32
6.70
10.80
12.90
17.60
21.70
26.40
31.80
37.78
45.00
53.80
65.20
80.90
103.50
x

#64 P-II-6 C-1

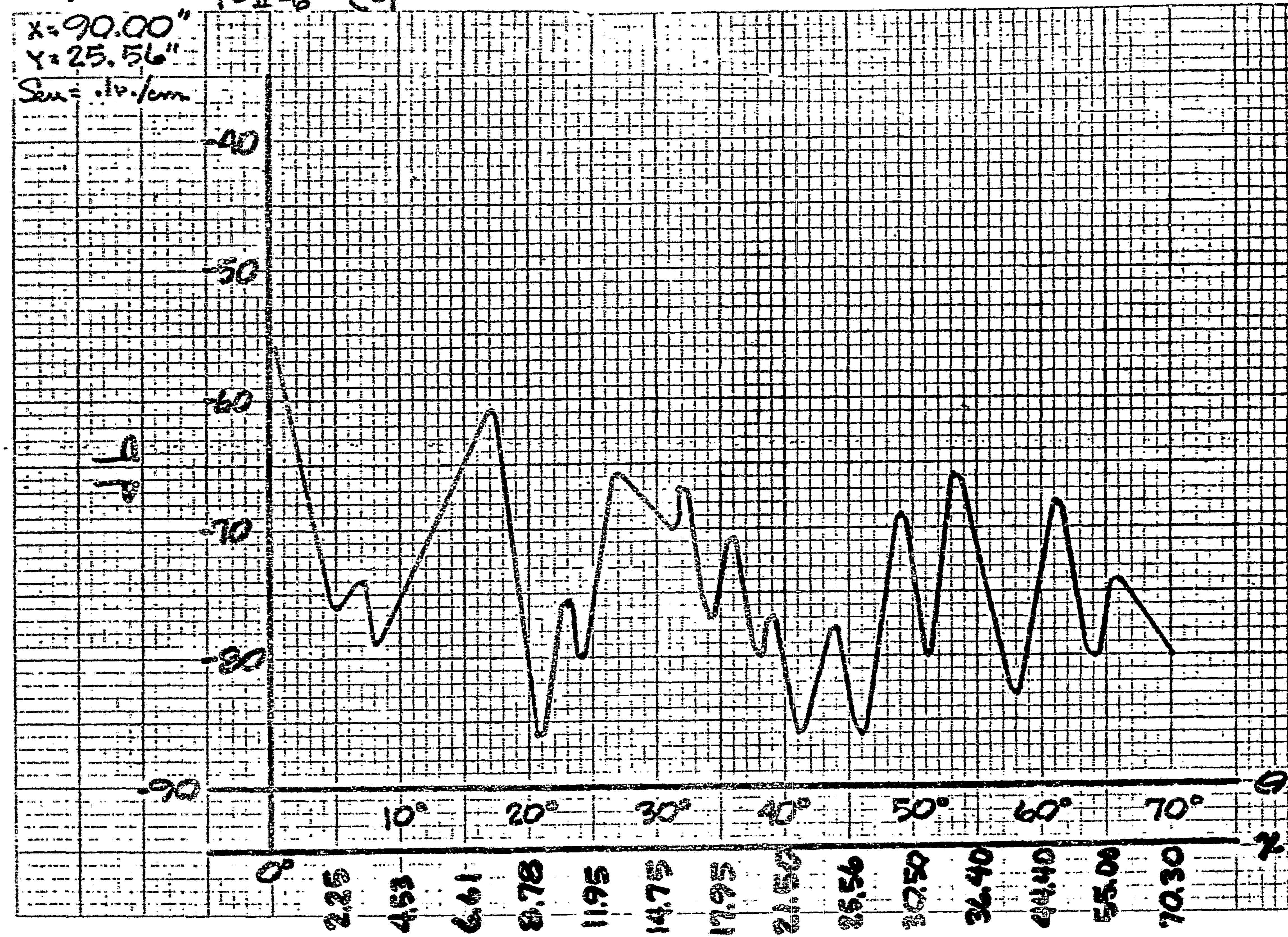

10 Squares to the Inch

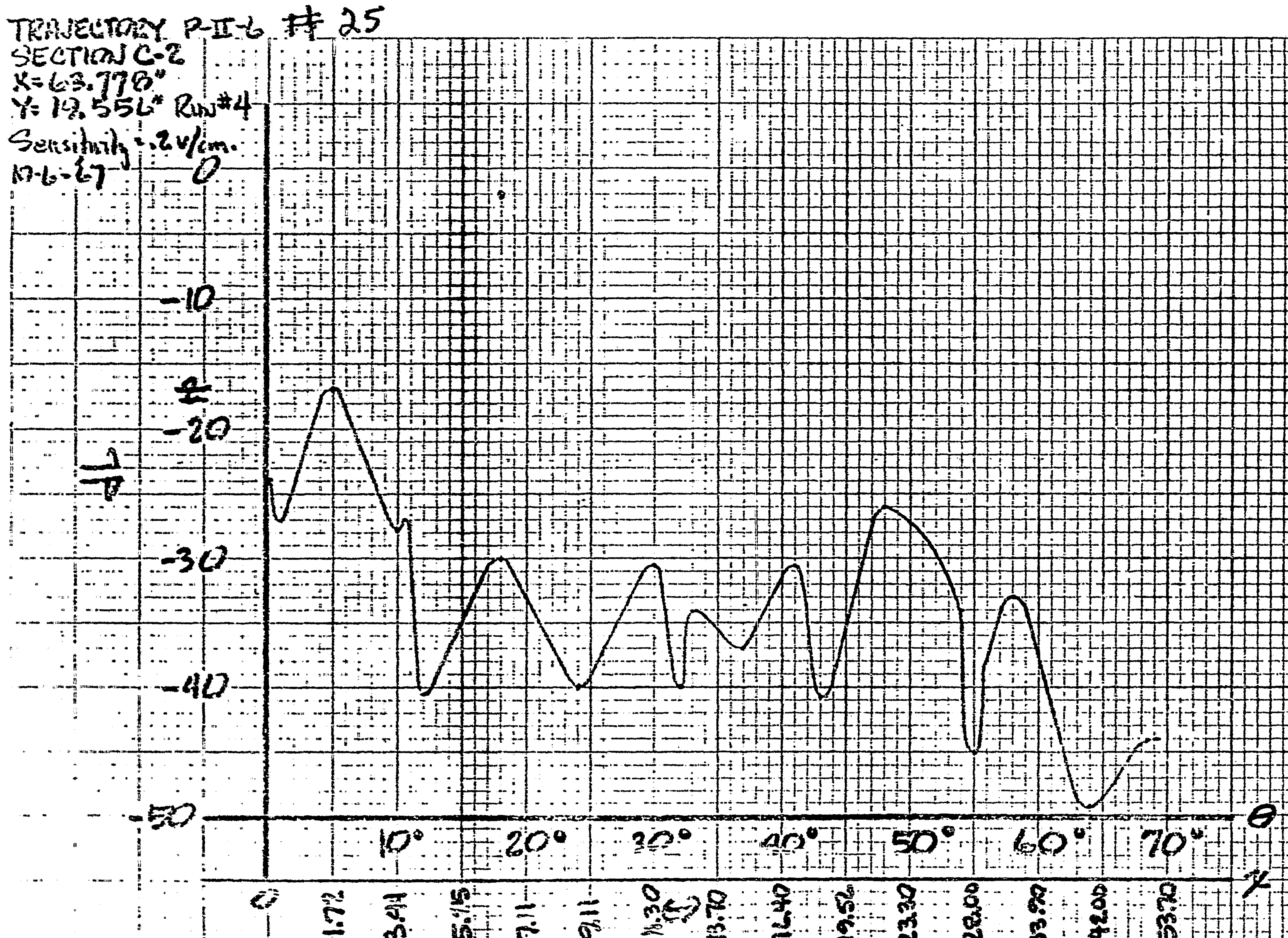

ares to the Inch

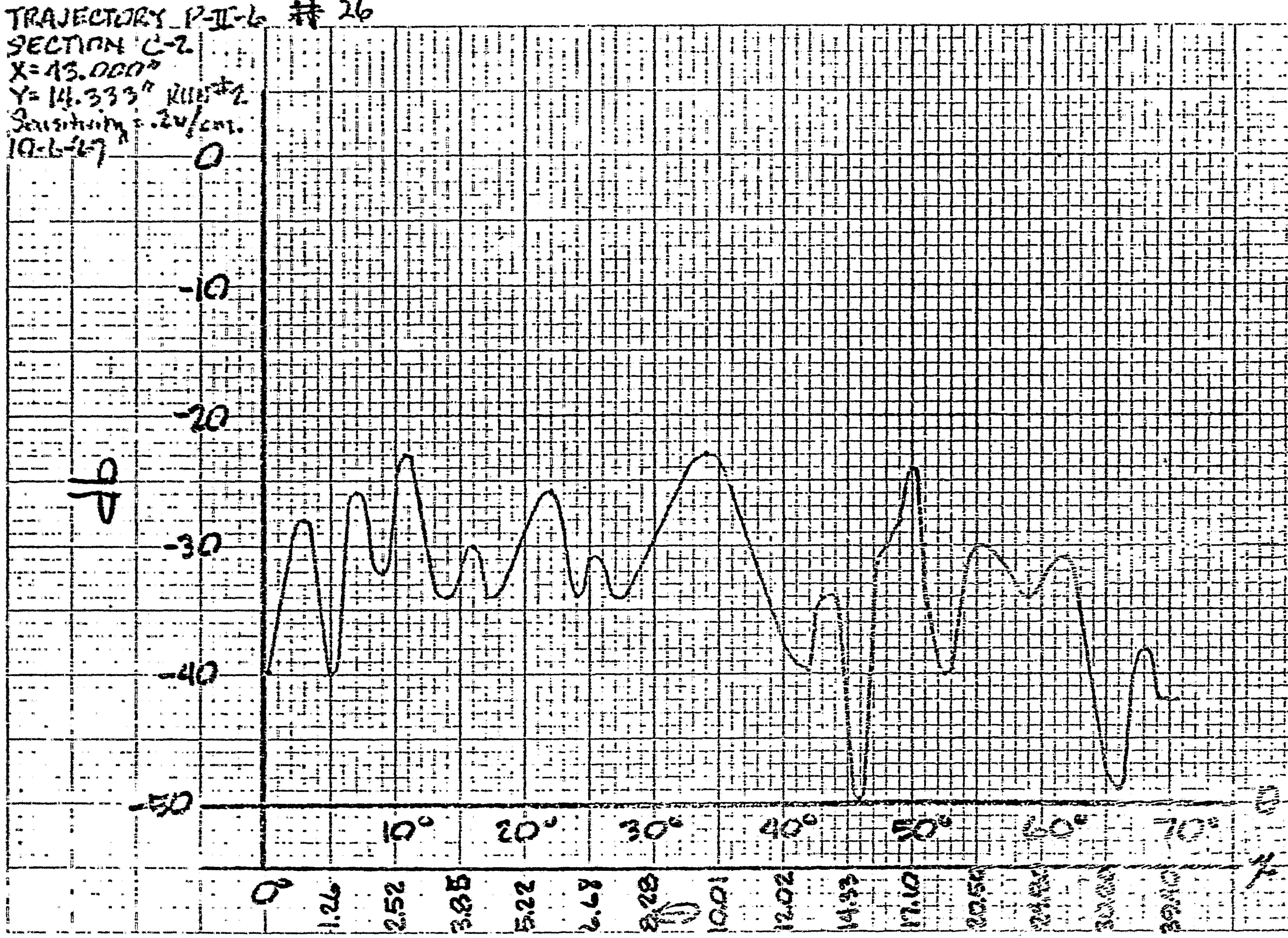
TRAJECTORY P-II-6 # 26
SECTION C-2
X=43.000"
Y=14.333" RUN #2
Sensitivity=.2v/cm.
10-6-67
0
-10
-20
-30
-40
-50
db
10°
20°
30°
40°
50°
60°
70°
0
1.26
2.52
3.85
5.22
6.68
8.28
10.01
12.02
14.33
17.10
20.50
24.85
30.80
39.40

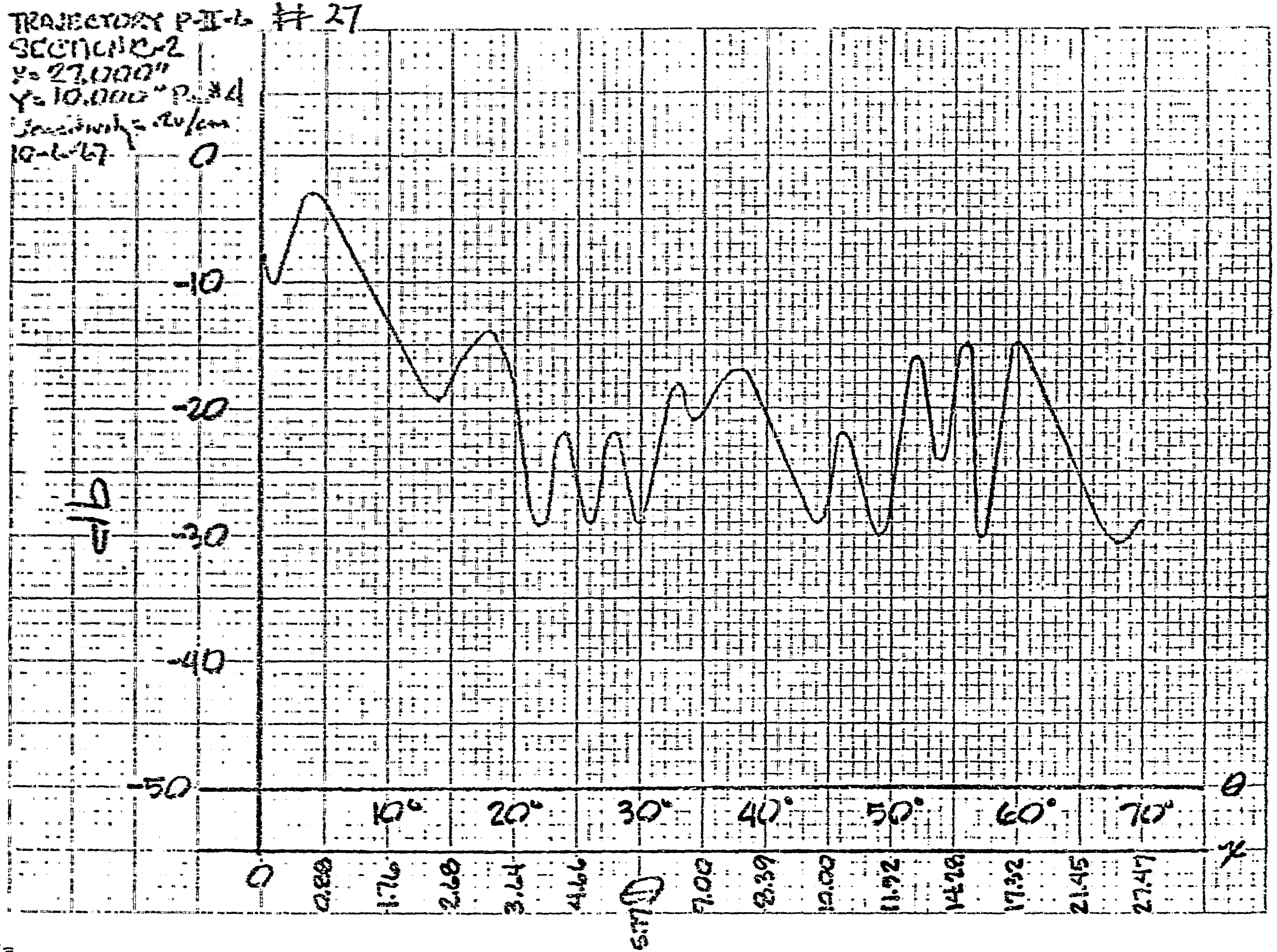

TRAJECTORY P-II-b #27
SECTION C-2
X= 27,000"
Y= 10,000" P=34
10-6-67
0
-10
-20
-30
-40
-50
10°
20°
30°
40°
50°
60°
70°
θ
0
0.88
1.76
2.68
3.64
4.66
5.77
7.00
8.39
10.00
11.92
14.28
17.32
21.45
27.47

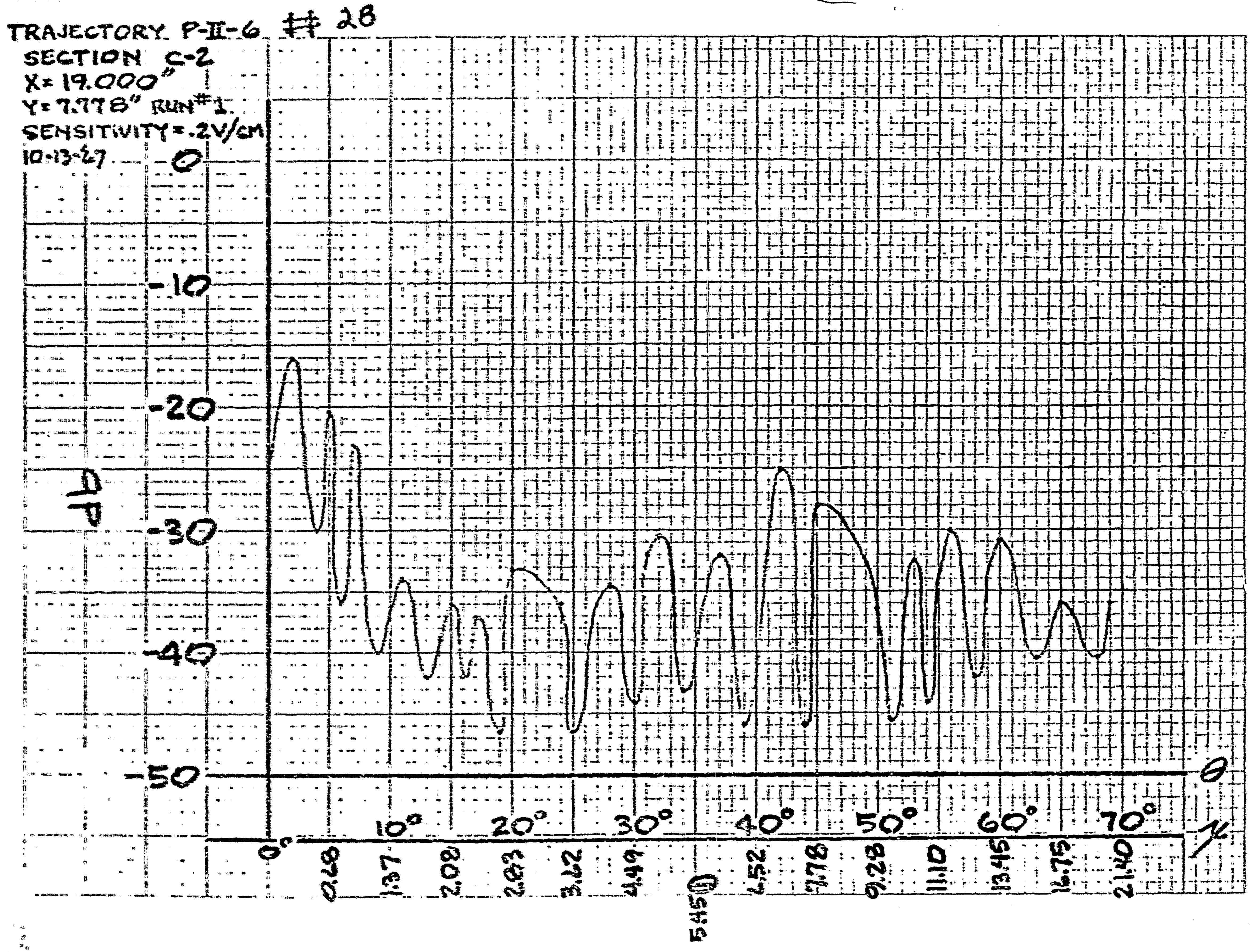
TRAJECTORY P-II-6 #28
SECTION C-2
X = 19.000"
Y = 7.778" RUN #1
SENSITIVITY = .2V/CM
10-13-47
dP
0
-10
-20
-30
-40
-50
0
0°
10°
20°
30°
40°
50°
60°
70°
0.68
1.37
2.08
2.83
3.62
4.49
5.45
6.52
7.78
9.28
11.10
13.45
16.75
21.40

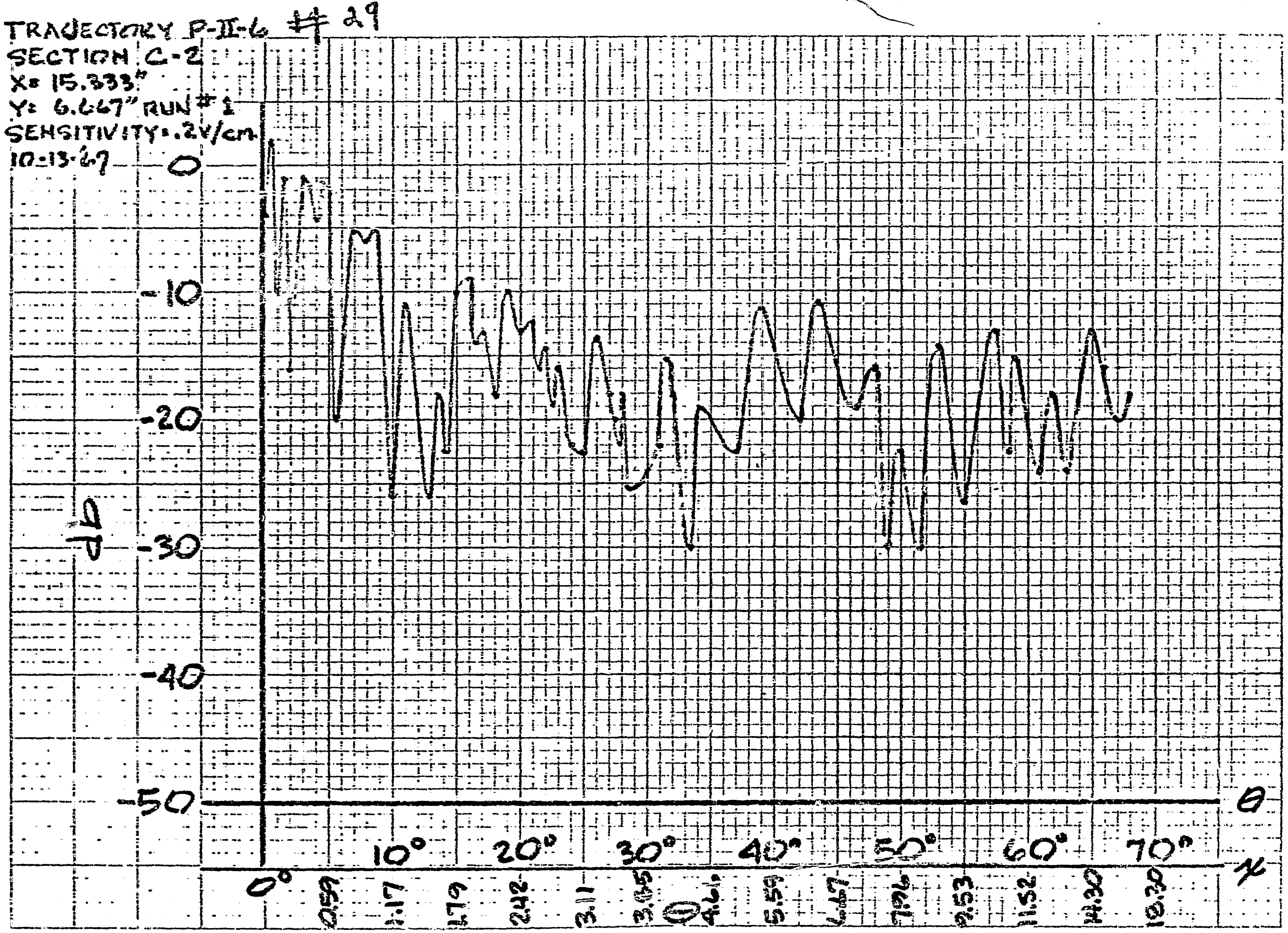

TRAJECTORY P-II-6 #29
SECTION C-2
X= 15.333"
Y: 6.667" RUN #1
SENSITIVITY: .2V/cm
10-13-67
0
-10
-20
-30
-40
-50
db
θ
0°
10°
20°
30°
40°
50°
60°
70°
x
0.59
1.17
1.79
2.42
3.11
3.65
4.61
5.59
6.67
7.96
9.53
11.52
14.30
18.30

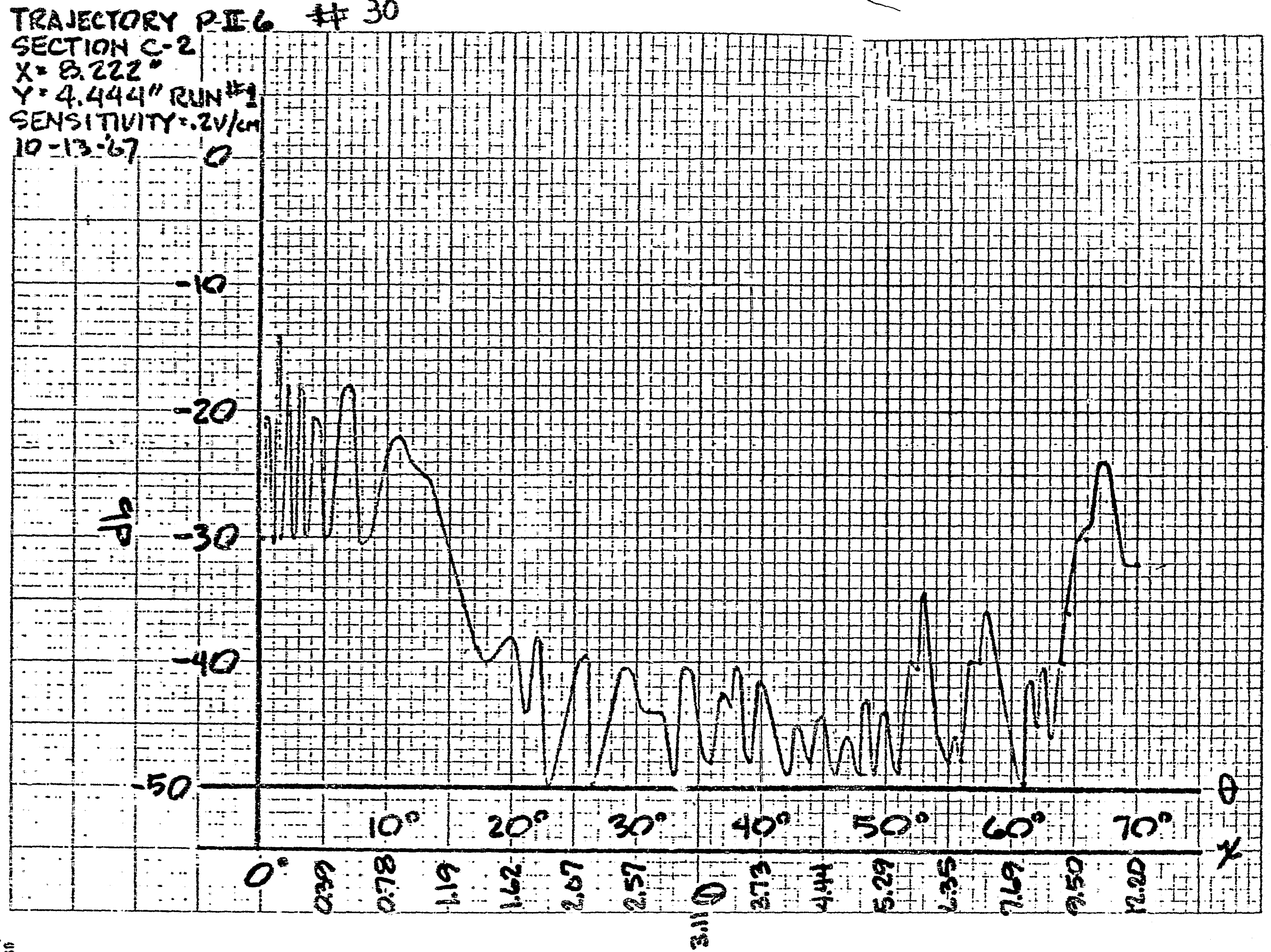

12-280

10 Squares to the Inch

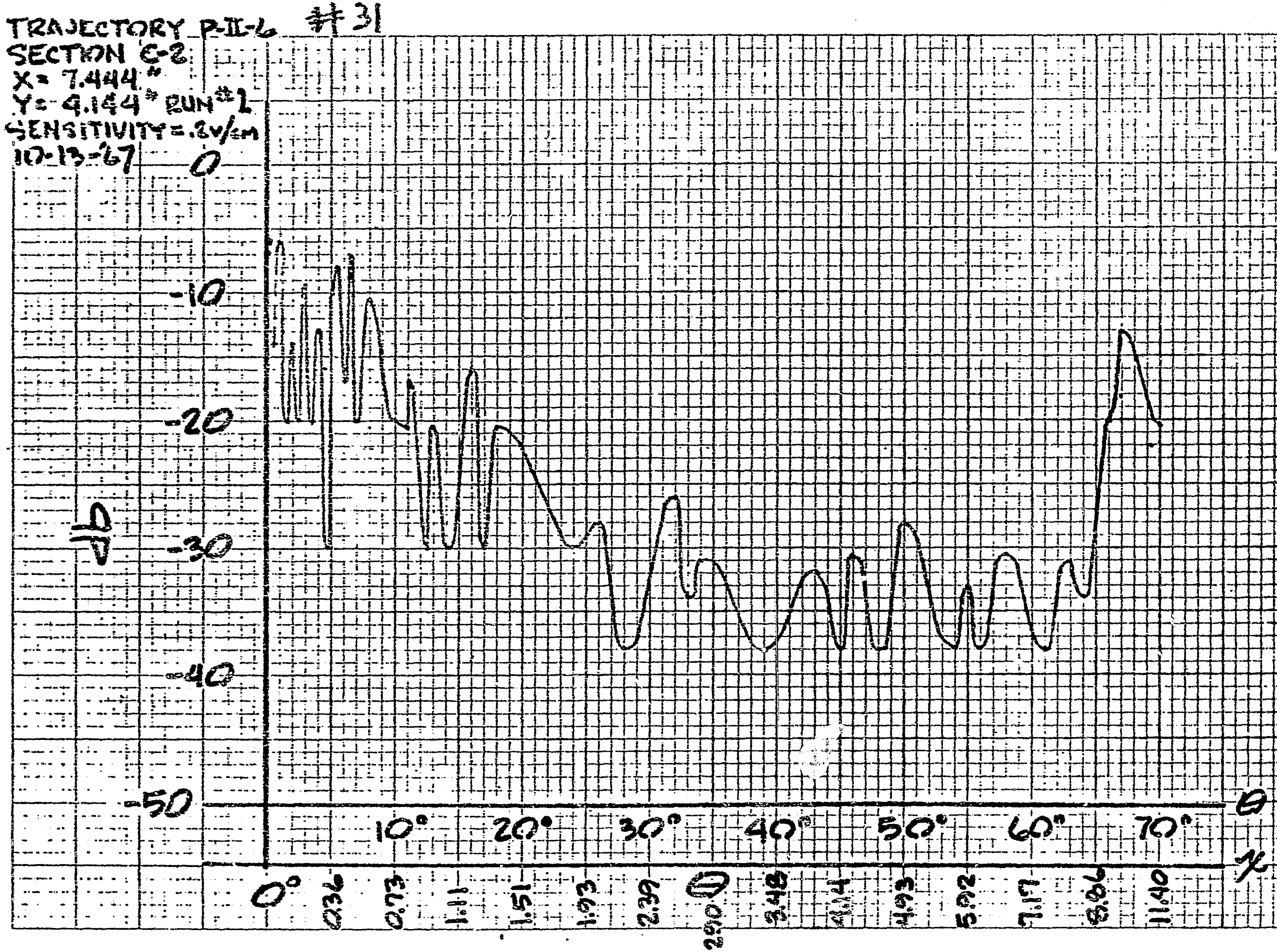

TRAJECTORY P-II-6 #31
SECTION C-2
X = 7.444"
Y = 4.144" RUN #1
SENSITIVITY = .2v/cm
10-13-67
0
-10
-20
-30
-40
-50
θ
10°
20°
30°
40°
50°
60°
70°
0°
0.36
0.73
1.11
1.51
1.93
2.39
2.90
3.48
4.14
4.93
5.92
7.17
8.86
11.40

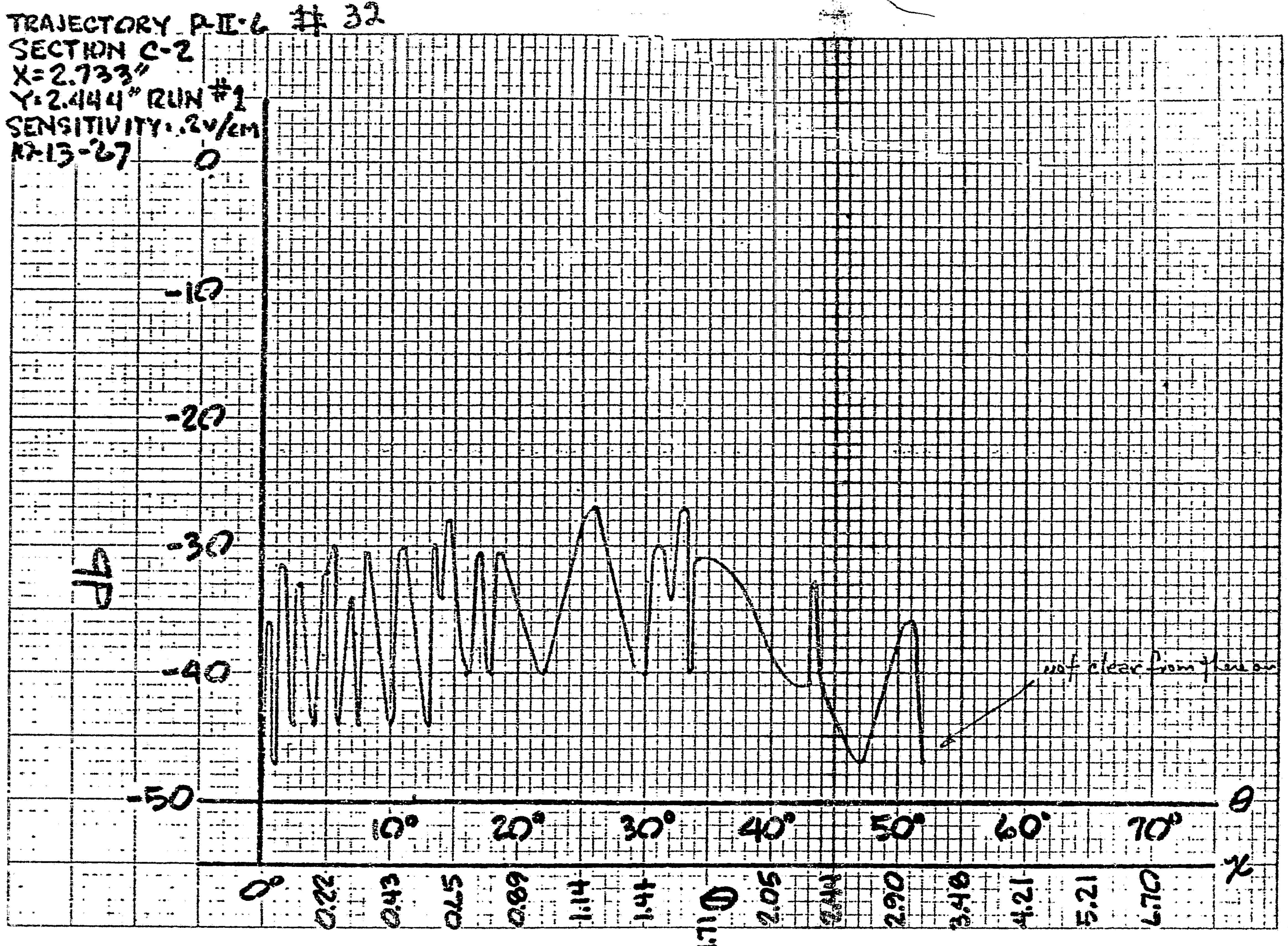

12-280

10 Squares to the Inch

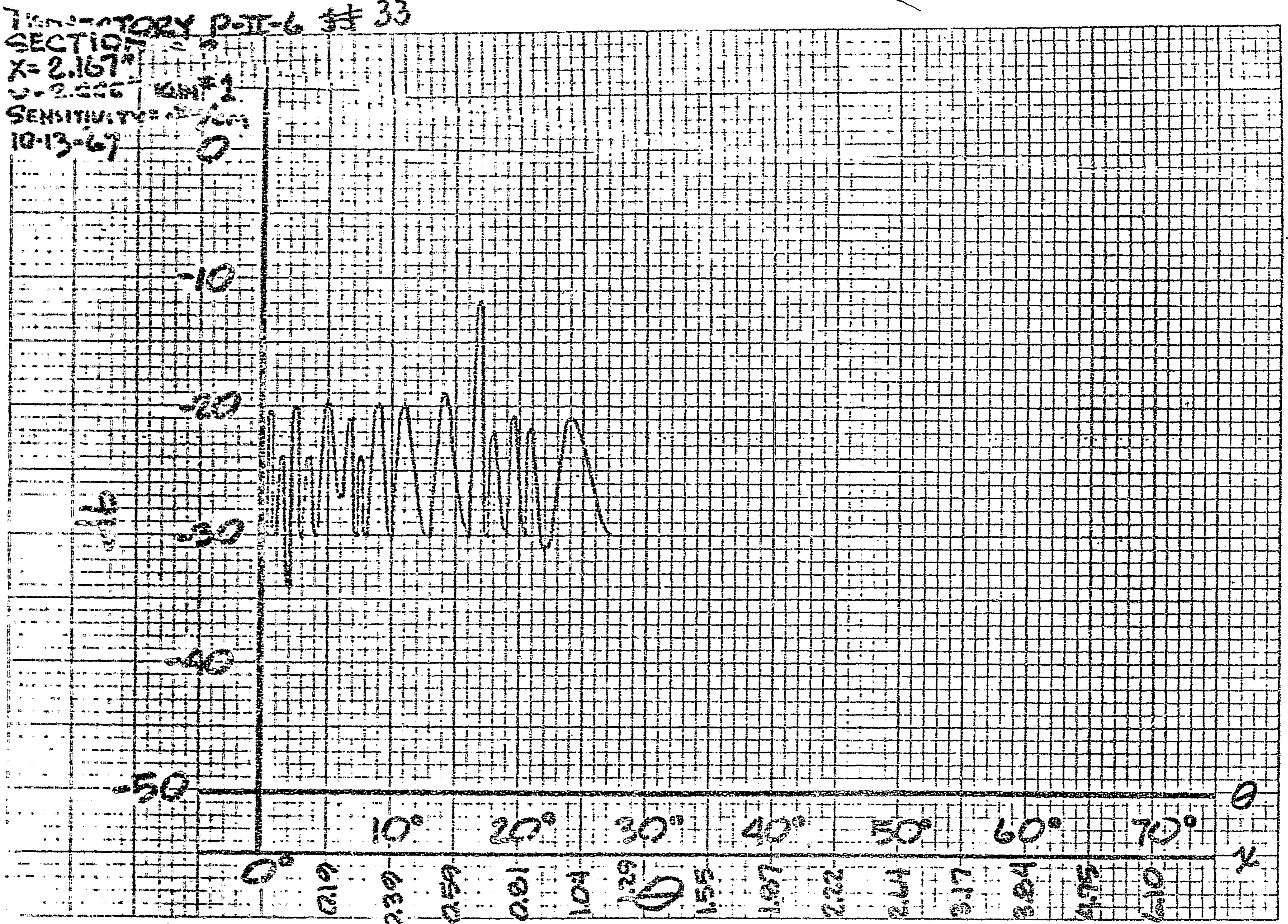

10 Squares to the Inch

Each plot of reflected field versus angle of incidence is plotted on a separate sheet with such details as altitude, distance from landing zone, and x,y positions on the model and model number. Each set of data was taken after the system was calibrated using flat plate model and repeatability of this data was assured before making these runs.

CONCLUSION

The LM acoustic simulation system has been carefully designed and built to avoid any extraneous vibration. The positioning and switching of all mechanical components have been operated and checked electronically to assure the continuity in the simulation process. Each set of data has been run and recorded repeatedly to the point until satisfactory comparison is made between runs. Therefore it is believed that optimum accuracy has been achieved within our scope upon the present existing system.

The return signal has also been re-examined point by point throughout the physical model. The curves agree favorably with predictions by the scattering theory. Any unexpected fluctuation caused by the frame iron angle near the edge of the model structure is pin-pointed. Such error, however, may be neglected and its real level may be interpreted from its neighboring data points.

REFERENCES

1. Hayre, H. S., F. Boyd and A. Tong. Ultrasonic Modeling of Lunar Approach of the Lunar Excursion Module. Technical Report TR-67-6, University of Houston, Wave Propagation Laboratory, Department of Electrical Engineering, March, 1967.

2. Hayre, H. S. "Acoustic Simulation of Lunar Echoes," Journal of Geophysical Research, Vol. 70, No. 16, pp. 3831-3839, 15 August 1965.

3. Beckman, P. and A. Spizzichino. The Scattering of Electromagnetic Waves From Rough Surfaces. New York: The Mac Millan Co., 1963.